Cellular/Molecular

NMDA Receptors Are Upregulated and Trafficked to the Plasma Membrane after Sigma-1 Receptor Activation in the Rat Hippocampus

Mohan Pabba,[1]* Adrian Y.C. Wong,[1]* Nina Ahlskog,[1] Elitza Hristova,[1] Dante Biscaro,[1] Wissam Nassrallah,[1] Johnny K. Ngsee,[2] Melissa Snyder,[1] Jean-Claude Beique,[2] and Richard Bergeron[1]

[1]Ottawa Hospital Research Institute, Ottawa, Ontario, Canada, K1H 8M5, and [2]Department of Cellular and Molecular Medicine, University of Ottawa, Ontario, Canada, K1H 8M5

Sigma-1 receptors (σ-1Rs) are endoplasmic reticulum resident chaperone proteins implicated in many physiological and pathological processes in the CNS. A striking feature of σ-1Rs is their ability to interact and modulate a large number of voltage- and ligand-gated ion channels at the plasma membrane. We have reported previously that agonists for σ-1Rs potentiate NMDA receptor (NMDAR) currents, although the mechanism by which this occurs is still unclear. In this study, we show that *in vivo* administration of the selective σ-1R agonists (+)-SKF 10,047 [2*S*-(2α,6α,11*R]-1,2,3,4,5,6-hexahydro-6,11-dimethyl-3-(2-propenyl)-2,6-methano-3-benzazocin-8-ol hydrochloride (*N*-allylnormetazocine) hydrochloride], PRE-084 (2-morpholin-4-ylethyl 1-phenylcyclohexane-1-carboxylate hydrochloride), and (+)-pentazocine increases the expression of GluN2A and GluN2B subunits, as well as postsynaptic density protein 95 in the rat hippocampus. We also demonstrate that σ-1R activation leads to an increased interaction between GluN2 subunits and σ-1Rs and mediates trafficking of NMDARs to the cell surface. These results suggest that σ-1R may play an important role in NMDAR-mediated functions, such as learning and memory. It also opens new avenues for additional studies into a multitude of pathological conditions in which NMDARs are involved, including schizophrenia, dementia, and stroke.**

Key words: **NMDA receptor; protein synthesis; sigma-1 receptor; surface biotinylation; trafficking; Western blot**

Introduction

Sigma receptors (σ-Rs) are widely expressed in the CNS and are involved in several physiological and pathological processes, such as neuronal firing, neurotransmitter release, learning and memory, neuroprotection, and drug abuse (for review, see Maurice and Su, 2009). Radioligand binding studies have suggested that two subtypes of σ-Rs exist, σ-1R and σ-2R (Quirion et al., 1992; Myers et al., 1994), but only the σ-1R has been cloned and investigated extensively. After activation by agonists, σ-1Rs translocate from the endoplasmic reticulum (ER) to the plasma membrane in which they modulate both voltage-gated (Lupardus et al., 2000; Aydar et al., 2002; Zhang and Cuevas, 2002, 2005; Tchedre et al., 2008; Johannessen et al., 2009; Zhang et al., 2009; Kinoshita et al., 2012) and ligand-gated (Martina et al., 2007; Zhang et al., 2011a, b) ion channels. Thus, they are ideally suited to regulate a variety of processes that may affect cellular function.

One ligand-gated ion channel known to be modulated by σ-1Rs is the NMDA receptor (NMDAR), a receptor involved in learning and memory processes (for review, see Kerchner and Nicoll, 2008) and implicated in cell death associated with neurological disorders, such as excitotoxicity and ischemia (Forder and Tymianski, 2009). Although the mechanism of interaction between σ-1Rs and NMDARs remains unclear (Martina et al., 2007; Balasuriya et al., 2013), it has been demonstrated that activation of σ-1Rs leads to potentiation of NMDAR-mediated responses in neurons (Monnet et al., 1990; Bergeron et al., 1995, 1996, 1997; Debonnel et al., 1996b; Martina et al., 2007; Zhang et al., 2011a,b). One possible avenue by which NMDARs are potentiated is via an increase in the number of receptors expressed at the plasma membrane. This could be attributable to either *de novo* protein synthesis or a redistribution of existing NMDARs (e.g., from intracellular pools to the plasma membrane).

Here we show that σ-1R activation, after an intraperitoneal injection of the σ-1R agonists (+)-SKF 10,047 [2*S*-(2α,6α,11*R**]-1,2,3,4,5,6-hexahydro-6,11-dimethyl-3-(2-propenyl)-2,6-methano-3-benzazocin-8-ol hydrochloride (*N*-allylnormetazocine) hydrochloride (SKF)], PRE-084 [2-morpholin-4-ylethyl 1-phenylcyclohexane-1-carboxylate hydrochloride (PRE)], or (+)-pentazocine (PTZ) (de Montigny et al., 1992; Monnet et al., 1994, 1996; Bergeron et al., 1995; Debonnel et al., 1996b) results in an

Received Feb. 1, 2014; revised July 8, 2014; accepted July 14, 2014.

Author contributions: M.P., A.Y.C.W., N.A., J.-C.B., and R.B. designed research; M.P., N.A., E.H., D.B., and W.N. performed research; M.P., A.Y.C.W., N.A., and E.H. analyzed data; M.P., A.Y.C.W., N.A., E.H., J.K.N., M.S., J.-C.B., and R.B. wrote the paper.

This work was supported by Canadian Institutes of Health Research Operating Grant MOP-79360 (R.B.) and Grant MOP-115062 (J.C.B.).

The authors declare no competing financial interests.

*M.P. and A.Y.C.W. contributed equally to this work.

Correspondence should be addressed to Richard Bergeron, Ottawa Hospital Research Institute, 451 Smyth Road, Roger Guindon Hall, Room 3501N, Ottawa, Ontario, Canada, K1H 8M5. E-mail: rbergeron@ohri.ca.

DOI:10.1523/JNEUROSCI.0458-14.2014

 0270-6474/14/3411325-14$15.00/0

increase in protein synthesis of the NMDAR subunits GluN2A and GluN2B along with postsynaptic density protein 95 (PSD-95). The selective σ-1R antagonists BD1047 (*N*′-[2-(3,4-dichlorophenyl)ethyl]-*N*,*N*,*N*′-trimethylethane-1,2-diamine) and BD1063 (1-[2-(3,4-dichlorophenyl)ethyl]-4-methylpiperazine) (Matsumoto et al., 1995; McCracken et al., 1999) abolish this effect. We also show an increased interaction between σ-1Rs and GluN2 subunits, as well as an increase in surface levels of NMDARs after σ-1R activation. This suggests a novel mechanism in which σ-1Rs regulate NMDAR expression and trafficking, potentially altering NMDAR function at the synapse.

Materials and Methods

Animals. Male Sprague Dawley rats (6–8 week old) were purchased from Charles River. They were acclimatized and housed under standard conditions and had access to standard chow and water *ad libitum*. The in-house σ-1R $^{-/-}$ mice (Langa et al., 2003) and their wild-type littermates were also housed under standard conditions. All procedures in this study were performed in accordance with the guidelines of the Canadian Council on Animal Care, which conform to National Institutes of Health guidelines, and were approved by the University of Ottawa Animal Care Committee. All animal procedures were performed under isoflurane anesthesia.

Antibodies. The following antibodies and their dilutions were used in this study: mouse monoclonal anti-GluN1 (1:10,000; Synaptic Systems); mouse monoclonal anti-GluN2A and mouse monoclonal anti-GluN2B (both 1:750; LifeSpan Biosciences); rabbit monoclonal anti-GluA1 clone C3T (1:2500; Millipore); rabbit polyclonal anti-GluA2/3/4 (1:3500; Cell Signaling Technology); mouse monoclonal anti-PSD-95 (1:10,000; Affinity BioReagents); and goat polyclonal anti-σ-1R (1:250; Santa Cruz Biotechnology). For sucrose-gradient fractionation and differential centrifugation controls, we used the following: mouse monoclonal anti-β-actin (1:14,000; GenScript); mouse monoclonal anti-BiP and rabbit polyclonal anti-Rab5a (1:2000 and 1:1000 respectively; Lifespan Biosciences); goat polyclonal anti-calnexin (C-20) and goat polyclonal anti-flotillin (both 1:250; Santa Cruz Biotechnology); rabbit polyclonal anti-clathrin and rabbit polyclonal anti-glycine receptor (GlyR; (1:5000 and 1:2000 respectively; Thermo Fisher Scientific); rabbit polyclonal anti-CREB (1:2000; Cell Signaling Technology); and rabbit polyclonal anti-nucleolin and rabbit polyclonal anti-β-tubulin (1:2000 and 1:30,000, respectively; Abcam). HRP-conjugated secondary antibodies were all purchased from Jackson ImmunoResearch.

Drugs. SKF, PRE, BD1047, and BD1063 were purchased from Tocris Cookson, PTZ was purchased from Sigma-Aldrich, and anisomycin was purchased from Bioshop. SKF, BD1047, and BD1063 were dissolved directly in PBS (in mM: 137 NaCl, 2.7 KCl, 10 Na_2HPO_4, and 1.8 KH_2PO_4, pH 7.4). PTZ was initially dissolved in warm 0.1N HCl and then diluted with PBS before use. Anisomycin was dissolved in DMSO and then diluted with PBS before use (final concentration was 20% DMSO).

Drug administration. Rats (4–6 weeks of age) were injected intraperitoneally with SKF, PTZ, or PRE (all 2 mg/kg) based on previously published reports (Steinfels et al., 1988; Miller et al., 1992; Beskid et al., 1998) or PBS for vehicle control. The hippocampi were collected 30, 45, or 90 min after injection because brain concentrations of PTZ are maximal ~20–30 min after injection and negligible after 120 min (Medzihradsky and Ahmad, 1971). We assumed similar pharmacokinetics for SKF and PRE. For σ-1R antagonist treatments, animals were either subcutaneously implanted with a 1 μl/h osmotic minipump (Alzet) containing BD1047 or BD1063 (both 2 $mg \cdot kg^{-1} \cdot d^{-1}$) for 2 d (chronic administration) to ensure steady-state antagonist concentration or injected intraperitoneally with 2 mg/kg for 1 h (acute) before σ-1R agonist administration. Although acute administration is sufficient to block σ-1Rs (Nguyen et al., 2005), we used chronic administration to take advantage of σ-1R downregulation observed after prolonged administration of BD1047 (Zambon et al., 1997). To inhibit protein synthesis, anisomycin (30 mg/kg) was injected intraperitoneally 1 h before SKF or PTZ treatment (Wanisch and Wotjak, 2008). In the case of *in vitro* experiments, hippocampal slices were preincubated with 50 μM BD1063 for 1 h before SKF (1 or 5 μM) treatment for 90 min.

Isolation of crude synaptosomal fractions. Differential centrifugation steps on control and drug-treated hippocampi were performed as described previously with minor modifications (Fig. 1*A*; Hallett et al., 2008). All steps were performed at 4°C. Briefly, isolated hippocampi were homogenized in homogenization buffer [20 mM Tris-HCl, 320 mM sucrose, 5 mM EDTA, 1 mM EGTA, 10 mM NaF, 2 mM Na_3VO_4, 1 mM PMSF, and 1× EDTA-free protease inhibitor cocktail (Roche), pH 7.4]. The total homogenate (TH) was centrifuged at 800 relative centrifugal force (rcf) for 10 min, and the resulting pellet (P1) and supernatant (S1) were collected. S1 was further centrifuged for 15 min at 9200 rcf to obtain the pellet (P2) and supernatant (S2). P2 was subjected to hyposmotic lysis by resuspension in 750 μl of homogenization buffer with 35.6 mM sucrose instead of 320 mM. The lysate was then incubated on ice for 30 min with occasional mixing before centrifugation at 25,000 rcf for 30 min. Both the resulting supernatant (LS1) and the pellet [crude synaptosomal membrane fraction (LP1)] were collected. The pellet was solubilized in 300 μl of solubilization buffer (20 mM Tris-HCl, 5 mM EDTA, 1 mM EGTA, 10 mM NaF, 2 mM Na_3VO_4, 1 mM PMSF, 1% NP-40, 0.1% SDS, 0.1% Na-deoxycholate, and 1× EDTA-free protease inhibitor cocktail, pH 7.4) for 30 min with end-over-end rotation and then subjected to a short spin for 5 min at 16,000 rcf. The resulting solubilized LP1 (crude synaptosomal fraction) was collected and diluted more than 10× for protein measurement. All the other isolated pellets were resuspended in homogenization buffer. The protein concentration of all isolated fractions was determined by Bradford assay (Bio-Rad) before resolving on SDS-PAGE and Western blot (WB).

Slice preparation. Coronal brain slices (300 μm thick) containing the hippocampus were obtained as follows: anesthetized rats were decapitated, and the brains were removed into ice-cold oxygenated (95% O_2/5% CO_2) artificial CSF [ACSF (in mM): 126 NaCl, 2.5 KCl, 2 $CaCl_2$, 1 $MgCl_2$, 26 $NaHCO_3$, and 10 glucose, pH 7.3 (300 mOsm)]. Slices were made using a vibrating microtome (Leica VT 1000S) and transferred to a six-well plate. SKF (1 or 5 μM) was added directly to the ACSF, and an equivalent amount of PBS was added to a control well. The slices were homogenized using Dounce homogenizer in homogenization buffer 90 min after SKF administration. The homogenate was then processed to obtain LP1 as above. Protein concentration was determined by Bradford assay before subjecting it to WB.

Subcellular fractionation. Subcellular fractionation was performed on hippocampi from vehicle- and drug-treated animals as described previously (Blackstone et al., 1992) with some modifications. All steps were performed at 4°C. LP1 fractions were obtained as described above and resuspended in homogenization buffer, layered on top of a discontinuous sucrose gradient containing 0.8 M/1.0 M/1.2 M sucrose, and centrifuged for 2 h at 65,000 rcf. Fractions at the 0.8 M/1.0 M [vesicular fraction (VF)] and 1.0 M/1.2 M interfaces [purified synaptosomal membrane fraction (SMF)] were collected, as well as the pellet fraction (PF). VF and SMF were separately cleared by centrifugation at 30,000 rcf for 30 min, and all the pellets were resuspended in 300 μl of homogenization buffer without sucrose before Bradford assay and WB.

Coimmunoprecipitation. P2 PFs were isolated as described above, and immunoprecipitation (Co-IP) experiments were performed as described previously (Suh et al., 2010) with some modifications. All steps were performed at 4°C unless otherwise stated. In short, P2 pellets were solubilized in 200–300 μl of lysis buffer (50 mM Tris-HCl, 2 mM EDTA, 0.5% Na-deoxycholate, and 1× EDTA-free protease inhibitor cocktail, pH 8.8) at 37°C for 30 min before dilution with 5 vol of ice-cold neutralization buffer (50 mM Tris-HCl, 2 mM EDTA, 0.1% Triton X-100, and 1× EDTA-free protease inhibitor cocktail, pH 6.8). The lysate was incubated with end-over-end rotation for 30 min and then centrifuged at 25,000 rcf for 30 min. Antibodies (σ-1R, PSD-95, GluN2A, or GluN2B) and prewashed Protein A/G-ultralink agarose resin (Pierce) were added to the supernatant at 5 μg of antibody per 400 μg of protein. After an overnight incubation with end-over-end rotation, the beads were collected by centrifugation at 1200 rcf for 5 min and then washed four times with ice-cold wash buffer (50 mM Tris-HCl, 50 mM NaCl, 2 mM EDTA, and 0.1% Triton X-100, pH 7.4), and the protein complexes were eluted by adding 5× SDS sample buffer. The specificity of σ-1R antibody was tested by incubating antibodies with blocking peptide [a short region of σ-1R C

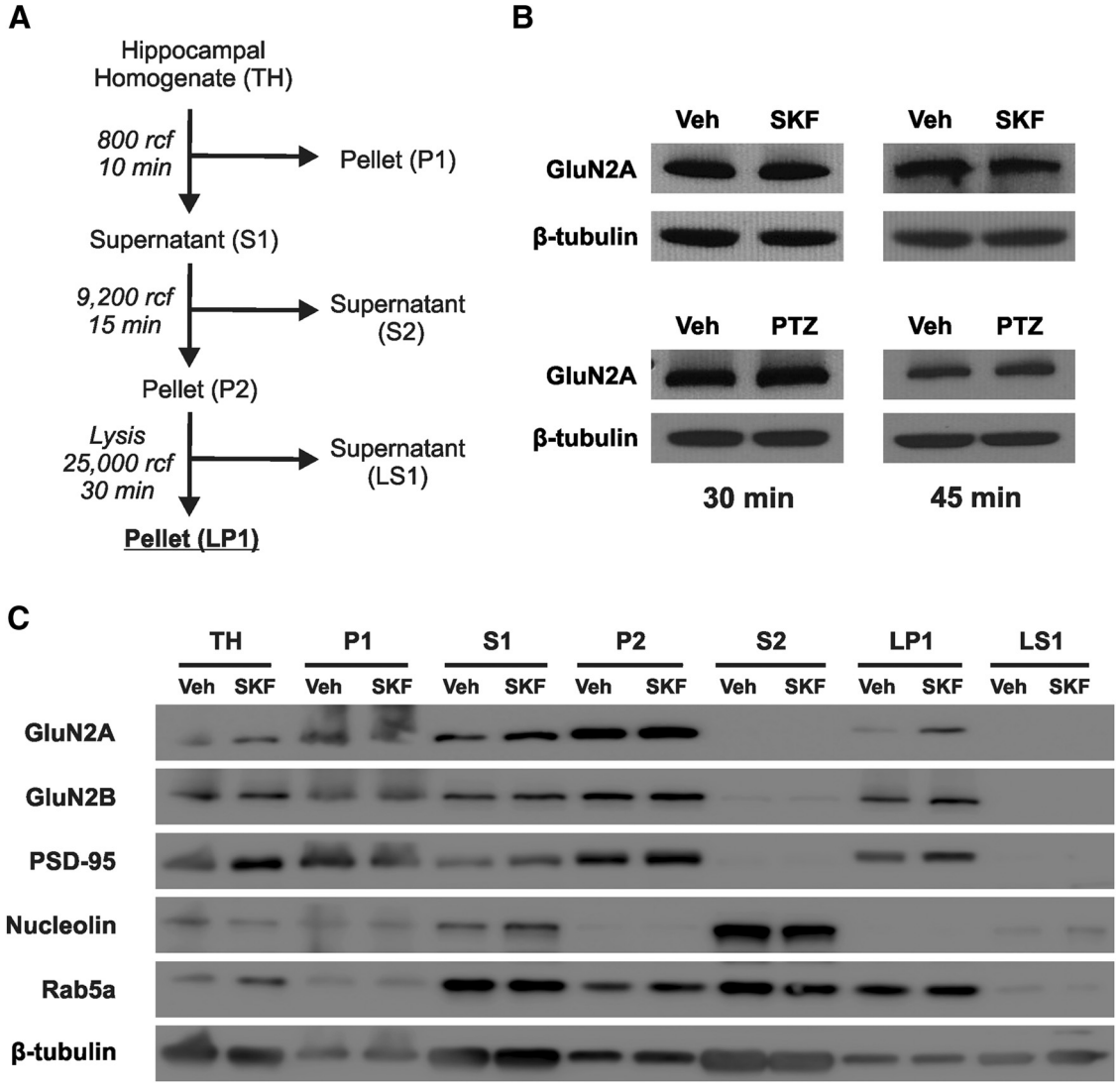

Figure 1. An increase in GluN2 subunit expression in the LP1 fraction is observed 90 min after σ-1R agonist administration. ***A***, Schematic diagram showing the methodology used to isolate subcellular fractions from hippocampal homogenate. ***B***, Representative WBs of LP1 probed for GluN2A expression 30 and 45 min after vehicle (Veh), SKF, or PTZ injection with β-tubulin as the loading control. ***C***, WBs of all the fractions depicted in ***A***. An upregulation of GluN2 subunits and PSD-95 is observed in LP1 after administration of SKF. Nucleolin and Rab5a were used as fraction controls and β-tubulin as the loading control. No change in nucleolin and Rab5a levels was observed after SKF treatment.

terminus (Santa Cruz Biotechnology)] at a ratio of 1:5 for overnight at 4°C before subjecting to WB for detecting σ-1Rs in P2 lysates from σ-1R $^{+/+}$ or σ-1R $^{-/-}$ mice.

Surface biotinylation. To perform these experiments, we followed the protocol published by Dennis et al. (2011) with some modifications. All steps were performed at 4°C unless otherwise stated. In brief, hippocampal slices (300 μm) from drug- and vehicle-treated rats were incubated with 0.5 mg/ml EZ-sulfo-NHS-SS-biotin (Pierce) in PBS for 20 min on ice to biotinylate surface proteins. Excess biotin was removed by washing the slices six times with cold supplemented Tris-buffered saline [TBS+ (in mM): 50 Tris-HCl, 150 NaCl, 20 $MgCl_2$, and 20 $CaCl_2$, pH 7.6] before homogenization in lysis buffer and sonicated for 20 s. Cell debris was removed by centrifugation for 10 min at 14,000 rcf and the supernatant (lysate) collected. The whole cell lysate was then incubated for 1 h with prewashed NeutrAvidin Agarose (Pierce) to capture biotinylated proteins. The beads were washed six times with 1 ml of TBS+ and two times with 1 ml of PBS containing 0.05% SDS. Bound proteins were recovered from the beads with 400 μl of elution buffer (50 mM Tris-HCl, 2% SDS, and 1 mM DTT, pH 6.8) by boiling for 10 min. Protein concentration was determined using DC assay (Bio-Rad) before SDS-PAGE and WB.

Western blotting and statistical analysis. For all WB samples, 10 μg of protein was resolved on 10% SDS-PAGE, transferred onto PVDF membranes, and developed using Luminata Crescendo (Millipore). Bands were detected using film or the LI-COR Odyssey Fc system (LI-COR Biosciences). Subsaturated bands were used for quantification of the pixel intensities using NIH ImageJ (Schneider et al., 2012) for films, and the Image Studio 2.0 software (LI-COR Biosciences) was used for collection and quantification when the LI-COR was used. WB experiments were repeated five to eight times from at least four different animals, and band intensities were normalized to β-tubulin or β-actin before comparison with vehicle unless otherwise stated. The statistical significance was determined using a two-tailed, unpaired Student's *t* test with a p value <0.05 considered statistically significant. The number of animals is represented by n.

Results

σ-1R activation increases hippocampal GluN2 subunit and PSD-95 expression

Agonist activation of σ-1Rs leads to an increase in NMDAR-mediated responses in the CNS (Monnet et al., 1990; Debonnel et

Table 1. Change in protein expression of NMDARs, AMPARs, and PSD-95 after SKF or PTZ administration

	(+)-SKF 10,047						(+)-Pentazocine					
	30 min		45 min		90 min		30 min		45 min		90 min	
	Veh	SKF	Veh	SKF	Veh	SKF	Veh	PTZ	Veh	PTZ	Veh	PTZ
GluN1	100 ± 19.3	105 ± 10.8	100 ± 1.35	88.6 ± 5.73	100 ± 20.5	118 ± 20.1	100 ± 7.57	109 ± 6.75	100 ± 8.91	90.3 ± 7.51	100 ± 10.2	98.7 ± 14.2
GluN2A	100 ± 3.45	100 ± 4.81	100 ± 13.2	122 ± 12.8	100 ± 12.2	263 ± 11.1*	100 ± 14.3	82.1 ± 12.6	100 ± 6.12	102 ± 9.02	100 ± 6.47	138 ± 6.57*
GluN2B	100 ± 10.7	100 ± 6.94	100 ± 13.6	109 ± 13.6	100 ± 13.8	260 ± 23.9*	100 ± 10.7	95.3 ± 9.97	100 ± 8.46	103 ± 8.65	100 ± 2.61	128 ± 2.93*
GluA1	100 ± 4.34	115 ± 6.75	100 ± 3.08	107 ± 3.66	100 ± 12.2	84.1 ± 2.81	100 ± 20.5	125 ± 22.6	100 ± 10.1	88.2 ± 11.8	100 ± 17.1	108 ± 14.3
GluA2/3/4	100 ± 6.57	101 ± 7.32	100 ± 5.03	95.2 ± 6.14	100 ± 11.8	97.6 ± 10.8	100 ± 14.8	105 ± 9.68	100 ± 7.98	101 ± 7.99	100 ± 18.2	95.7 ± 16.2
PSD-95	100 ± 8.02	119 ± 5.31	100 ± 2.06	94.2 ± 4.66	100 ± 12.1	188 ± 20.1*	100 ± 7.21	107 ± 9.68	100 ± 6.56	109 ± 7.81	100 ± 10.1	153 ± 9.42*

Columns showing values 30, 45, and 90 min after injection are expressed as a percentage of the corresponding vehicle with the experiments done in parallel. Data are mean ± SEM of at least four animals. *$p < 0.05$, significantly different from vehicle (Student's two-tailed, unpaired *t* test).

al., 1996a,b; Bergeron et al., 1997), but the mechanism by which this occurs is currently unclear. Although there are several possibilities that could explain this phenomenon, we chose to focus on two. First, σ-1R activation may lead to an increase in the number of cell-surface NMDARs. Second, σ-1R activation may mediate changes in NMDAR trafficking resulting in a redistribution of NMDARs (e.g., from the ER/Golgi to the plasma membrane) without a change in overall numbers.

Thus, our initial experiments focused on whether σ-1R activation affects the expression levels of NMDAR subunits in the LP1 (synaptosomal) fraction (Fig. 1*A*) after σ-1R activation *in vivo*. Although differential centrifugation is a widely used technique to isolate subcellular fractions, one technical limitation of this method is the potential for cross-contamination. We sought to address this problem by investigating the expression of marker proteins in all isolated fractions (Fig. 1*C*). Probing the crude fractions for NMDAR subunits and PSD-95 revealed enrichment in LP1, as well as the preceding fractions. Neither NMDARs nor PSD-95 were detected in the crude cytosolic (S2) or vesicle-enriched (LS1) fractions (Fig. 1*C*). Nucleolin, a cytosolic/nuclear DNA-binding protein, was enriched in the cytosolic fractions S2 and S1 as reported previously (Taha et al., 2014), and the early endosomal protein Rab5a was enriched in LP1 but not LS1 (Fischer von Mollard et al., 1994). Therefore, we are confident that the LP1 fractions isolated using differential centrifugation used in this study are not cross-contaminated.

Because there are many confounding pharmacokinetic factors that could affect the bioavailability of σ-1R agonists after intraperitoneal injection (e.g., blood–brain barrier permeability), we performed a time course experiment in which we collected tissue samples at three different time points after agonist injection. A representative WB for GluN2A at 30 and 45 min after administration of 2 mg/kg SKF (top), PTZ (bottom), or vehicle (PBS) is shown in Figure 1*B*. An intraperitoneal injection of SKF resulted in no change in expression level of any NMDAR under investigation 30 or 45 min after injection (Fig. 1*B*, Table 1: GluN2A, 100 ± 4.8%, $p = 0.98$ at 30 min and 122 ± 12% compared with vehicle, $p = 0.46$ at 45 min after injection, $n = 5$). Similar results were obtained when the experiments were repeated after PTZ injection (Fig. 1*B*: GluN2A, 82.1 ± 12%, $p = 0.37$ at 30 min and 102 ± 9% of vehicle, $p = 0.90$ at 45 min after injection, $n = 5$).

In contrast, a robust upregulation of GluN2A and GluN2B subunit expression was observed 90 min after SKF and PTZ injection (Fig. 1*B*). Injection of SKF results in a 263 ± 11% increase in GluN2A and a 260 ± 23% increase in GluN2B relative to vehicle (Fig. 2*A*,*B*: $p < 0.05$, $n = 5$). A σ-1R induced upregulation of PSD-95, a PSD protein associated with GluN2A and GluN2B subunits (Kornau et al., 1995; Niethammer et al., 1996), was also observed 90 min after SKF administration (Fig. 2*A*,*B*: 188 ± 20% of vehicle, $p < 0.05$, $n = 5$). Thus, σ-1R activation leads to significant upregulation of GluN2 subunits and PSD-95 90 min after agonist administration, and as a result, we performed all subsequent experiments at this time point.

To confirm that this upregulation was attributable to σ-1R activation, we repeated the experiment with two other σ-1R agonists, PRE and PTZ. As expected, intraperitoneal administration of 2 mg/kg PRE resulted in an increase in GluN2 subunits and PSD-95 expression (Fig. 2*C*: GluN2A, 146 ± 8.9%; GluN2B, 134 ± 9.7%; PSD-95, 121 ± 5.2% of vehicle, $p < 0.05$, $n = 6$). A similar increase was observed after PTZ injection (Fig. 2*D*: GluN2A, 138 ± 6.5%; GluN2B, 128 ± 2.9%; PSD-95, 153 ± 9.4% of vehicle, $p < 0.05$, $n = 5$). With both PRE and PTZ, the increase was less pronounced than with SKF. Surprisingly, we observed no change in the GluN1 expression level after SKF (Fig. 2*A*,*B*: 110 ± 8.3% of vehicle, $p = 0.44$, $n = 5$), PRE (Fig. 2*C*: 131 ± 27% of vehicle, $p = 0.41$, $n = 6$), or PTZ (Fig. 2*D*: 98.7 ± 14.2% of vehicle, $p = 0.76$, $n = 5$) injection. Therefore, activation of σ-1Rs by any one of three classical σ-1R agonists results in an upregulation of GluN2 subunits and PSD-95.

Previous studies have demonstrated that administration of σ-1R agonists has no significant effect on AMPA receptor (AMPAR)-mediated currents (Fletcher et al., 1995). One implication of this work is that the protein expression of AMPARs is not affected after σ-1R activation. To test this, we examined the levels of the AMPAR subunits GluA1 and GluA2/3/4 (Table 1). Our results revealed no significant changes in the levels of AMPAR subunits 90 min after an intraperitoneal injection of either SKF (Fig. 2*E*,*F*: GluA1, 84.2 ± 2.8%, $p = 0.32$; GluA2/3/4, 97.6 ± 11% of vehicle, $p = 0.91$, $n = 6$), PRE (Fig. 2*G*: GluA1, 109 ± 12%, $p = 0.71$; GluA2/3/4, 86.5 ± 19% of vehicle, $p = 0.35$, $n = 6$), or PTZ (Fig. 2*H*: GluA1, 108 ± 14%, $p = 0.80$; GluA2/3/4, 95.7 ± 16% of vehicle, $p = 0.91$, $n = 6$). Together, we show that administration of σ-1R agonists lead to an increase in protein levels of the NMDAR subunits GluN2A and GluN2B and PSD-95, but with no effect on AMPARs.

One confounding factor with *in vivo* injections of σ-1R agonists is the possibility of systemic effects of the drugs, given the widespread distribution of σ-1Rs (Matsumoto, 2007). To assess this, we cut 300-μm-thick hippocampal slices (see Materials and Methods) and then bath administered SKF to the slices *in vitro*. We used two different concentrations of SKF, 1 and 5 μM, both of which result in minimal NMDAR blockade (Fletcher et al., 1995) but produce maximal σ-1R binding (Gundlach, 1986). We then probed for GluN2 subunits and PSD-95 expression 90 min after SKF application. Both 1 and 5 μM SKF resulted in an upregulation of GluN1 (Fig. 3*A*,*B*: 1 μM SKF, 127 ± 2.1%; 5 μM SKF, 119 ± 10% of control, $p < 0.05$, $n = 4$) and GluN2A (Fig. 3*A*,*B*:

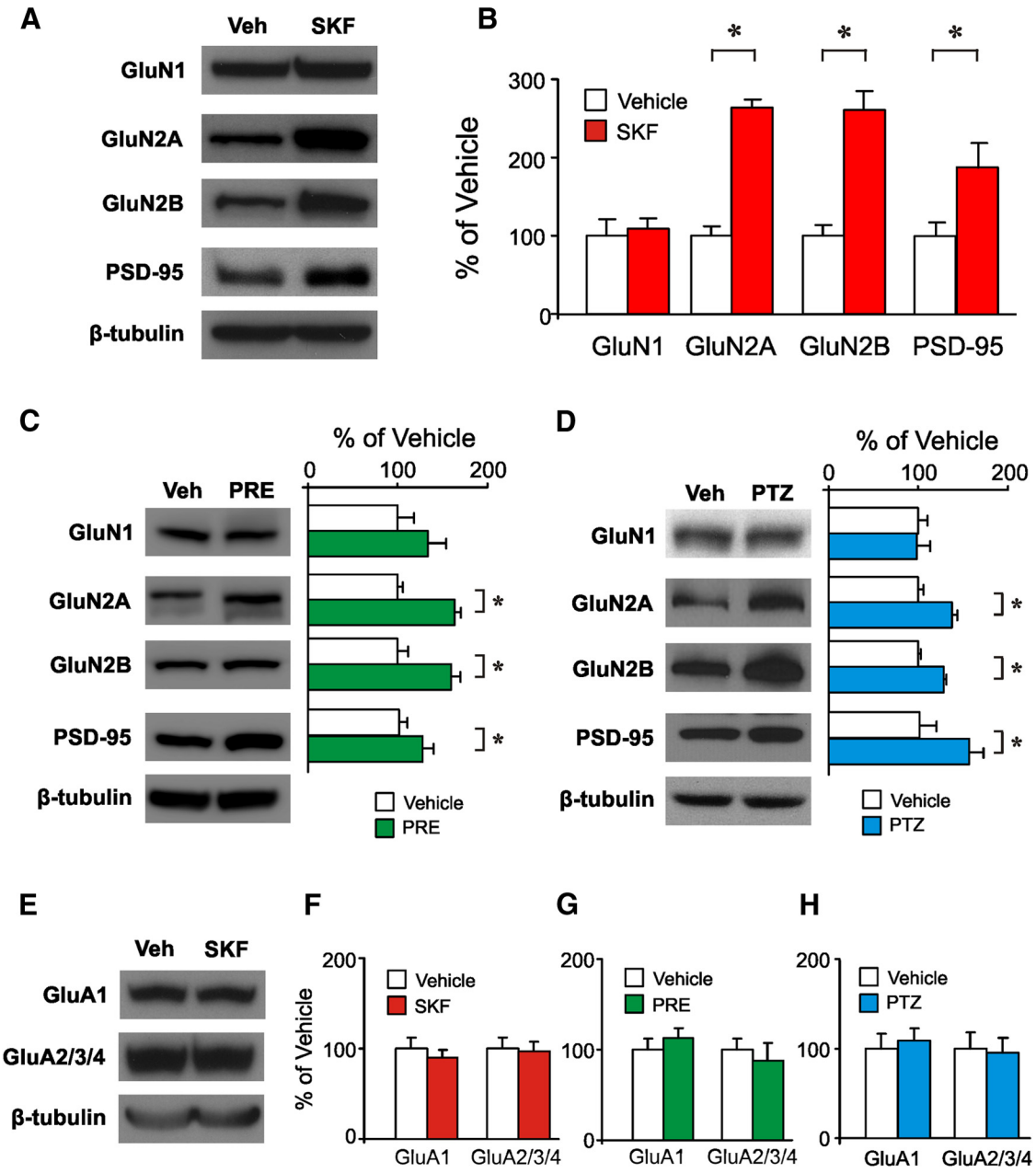

Figure 2. Injection of σ-1R agonists leads to an increase in GluN2 subunits and PSD-95 expression. A significant increase in protein expression of GluN2A, GluN2B, and PSD-95 was observed 90 min after intraperitoneal injection of vehicle (Veh) or SKF (***A***, ***B***). Similar results were obtained 90 min after injection of PRE (***C***) or PTZ (***D***). There was no change in the expression level of AMPARs after SKF (***E***, ***F***), PRE (***G***), or PTZ (***H***) injection. Bar graphs are mean ± SEM of at least five animals. *$p < 0.05$.

1 μM SKF, 125 ± 2.8%; 5 μM SKF, 112 ± 1.9% of control, $p < 0.05$, $n = 4$) subunits. A significant upregulation of GluN2B subunits was observed after bath application of 1 μM SKF (Fig. 3*A*,*B*: 110 ± 1.1% of control, $p < 0.05$, $n = 4$) but GluN2B was surprisingly downregulated after application of 5 μM SKF (Fig. 3*A*,*B*: 84 ± 4.7% of control, $p < 0.05$, $n = 4$). There was no significant change in PSD-95 expression after 1 μM SKF application (Fig. 3*A*,*B*: 112 ± 4.7%, $p = 0.07$, $n = 4$), but a significant increase in PSD-95 expression was observed after bath application of 5 μM SKF (Fig. 3*A*,*B*: 121 ± 3.9%, $p < 0.05$, $n = 4$). Thus, we show that the *in vivo* effects of σ-1R agonists are also observed in acute slices, demonstrating that the increase in GluN2 subunit and PSD-95 expression observed 90 min after agonist administration is attributable to σ-1R activation rather than any nonspecific systemic effects.

Upregulation of GluN2 subunits and PSD-95 protein expression is blocked by σ-1R antagonists

To verify that the increase in GluN2 subunits and PSD-95 that we see after SKF, PRE, or PTZ treatment is attributable to activation of σ-1Rs, we used the classical σ-1R antagonists BD1047 and BD1063 (Matsumoto et al., 1995). In our initial *in vitro* experiments, we bath applied 50 μM BD1063 to hippocampal slices 1 h before 1 μM SKF was applied in the continued presence of BD1063. Administration of BD1063 alone did not lead to any changes in NMDAR subunit or PSD-95 expression (Fig. 3*C*,*D*: GluN1, 111 ± 3.2% of vehicle, $p = 0.31$; GluN2A, 119 ± 16%, $p = 0.36$; GluN2B, 91 ± 6.1%, $p = 0.52$; PSD-95, 121 ± 7.6% of control, $p = 0.12$, $n = 5$). However, preincubation of BD1063 abolished the SKF-induced increase in NMDAR subunits (Fig. 3*C*,*D*: GluN1, 117 ± 10%, $p = 0.16$; GluN2A, 109 ± 8.1%, $p =$

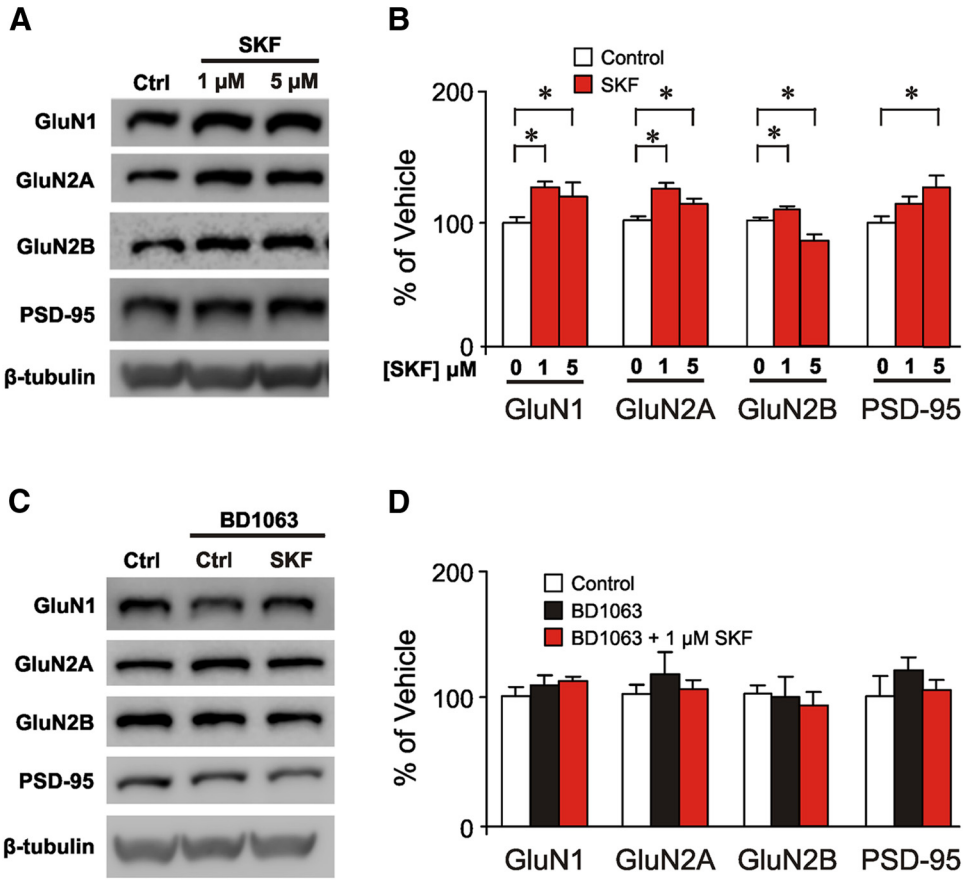

Figure 3. The increase in NMDAR subunit and PSD-95 expression is also observed after σ-1R activation in hippocampal slices. ***A***, WBs showing the protein level of GluN1, GluN2A, GluN2B, and PSD-95 after a 90 min bath application of 1 or 5 μM SKF. ***B***, A significant increase in GluN1, GluN2A, and GluN2B expression (relative to control; Ctrl) was observed in the presence of 1 μM SKF. A significant increase in PSD-95 expression was observed after application of 5 μM SKF. ***C***, ***D***, The increase in NMDAR and PSD-95 protein levels was abolished after pretreatment with 50 μM BD1063. Bar graphs are mean ± SEM of slices from at least five animals per treatment.

Table 2. Both acute and chronic administration of σ-1R antagonists block the increase in GluN2 subunit and PSD-95 observed after SKF, PTZ, or PRE administration

	Acute administration (2 mg/kg, i.p.)				Chronic administration (2 mg · kg^{-1} · d^{-1}, 2 d osmotic minipumps)				
	BD1047 (% of vehicle)		BD1063 (% of vehicle)		BD1047 (% of vehicle)			BD1063 (% of vehicle)	
	BD	SKF + BD	BD	PRE + BD	BD	SKF + BD	PTZ + BD	BD	SKF + BD
GluN2A	126 ± 11%	114.7 ± 7.8%	91 ± 7.1%	94 ± 4.8%	111 ± 4.2%	128 ± 14%	101 ± 14.2%	101 ± 6.1%	88 ± 6.2%
GluN2B	104 ± 3.3%	104 ± 9.6%	95 ± 0.8%	111 ± 9%	97.5 ± 4.0%	118 ± 6.5%	118 ± 16%	109 ± 10.2%	88 ± 10%
PSD-95	124 ± 44%	71 ± 14%	87 ± 1.8%	105 ± 0.75%	93 ± 5.8%	78 ± 14%	105 ± 2.0%	110 ± 13%	101 ± 3.8%

Data are mean ± SEM of at least four animals. No significant difference in protein levels was observed in all cases ($p > 0.05$, Student's two-tailed, unpaired *t* test).

0.55; GluN2B, 81 ± 8.4% of vehicle, $p = 0.12$, $n = 5$) and PSD-95 levels (PSD-95, 104 ± 9.5% of vehicle, $p = 0.69$, $n = 5$). Thus, the upregulation of NMDAR subunits and PSD-95 observed after σ-1R agonist administration is blocked by BD1063 in acute slices, confirming that activation of σ-1Rs underpins this phenomenon.

We then repeated the BD1063 experiments *in vivo* to verify what we observed in acute slices. For these experiments, rats were implanted with osmotic minipumps and infused with the antagonist BD1063 (2 mg · kg^{-1} · d^{-1}) for 2 d to ensure that σ-1Rs were blocked before challenging with SKF or PTZ (Table 2). No obvious behavioral phenotype was observed in BD1063-treated animals. Chronic BD1063 treatment alone had no effect on GluN2 subunit and PSD-95 expression levels (GluN2A, 101 ± 11%, $p = 0.90$; GluN2B, 109 ± 10%, $p = 0.74$; PSD-95, 110 ± 13%, of vehicle, $p = 0.13$, $n = 3$). As expected, pretreatment with BD1063 abolished the SKF-mediated increase in GluN2 subunits and PSD-95 expression (Table 2: GluN2A, 88 ± 6.2%, $p = 0.67$; GluN2B, 88 ± 10%, $p = 0.60$; PSD-95, 101 ± 3.8% of vehicle, $p = 0.86$, $n = 3$).

To confirm the data we obtained *in vivo* with BD1063, we repeated the experiment with another σ-1R antagonist BD1047 (Matsumoto et al., 1995). Because acute (intraperitoneal) administration of BD1047 results in effective σ-1R blockade (Nguyen et al., 2005), we compared the two routes of σ-1R antagonist administration (acute vs chronic) using 2 mg/kg BD1047. One experimental group received BD1047 for 2 d using osmotic minipumps (chronic), whereas the other group received a single intraperitoneal injection of BD1047 (acute) 1 h before σ-1R agonist injection. Figure 4*A* shows representative blots of NMDAR and PSD-95 expression after chronic and acute administration of BD1047 *in vivo*. Chronic antagonist treatment alone did not elicit a change in the protein levels under investigation (Fig. 4*A*,*B*, Table 2: GluN2A, 111 ± 4.2%, $p = 0.25$; GluN2B, 97.5 ± 4.0%,

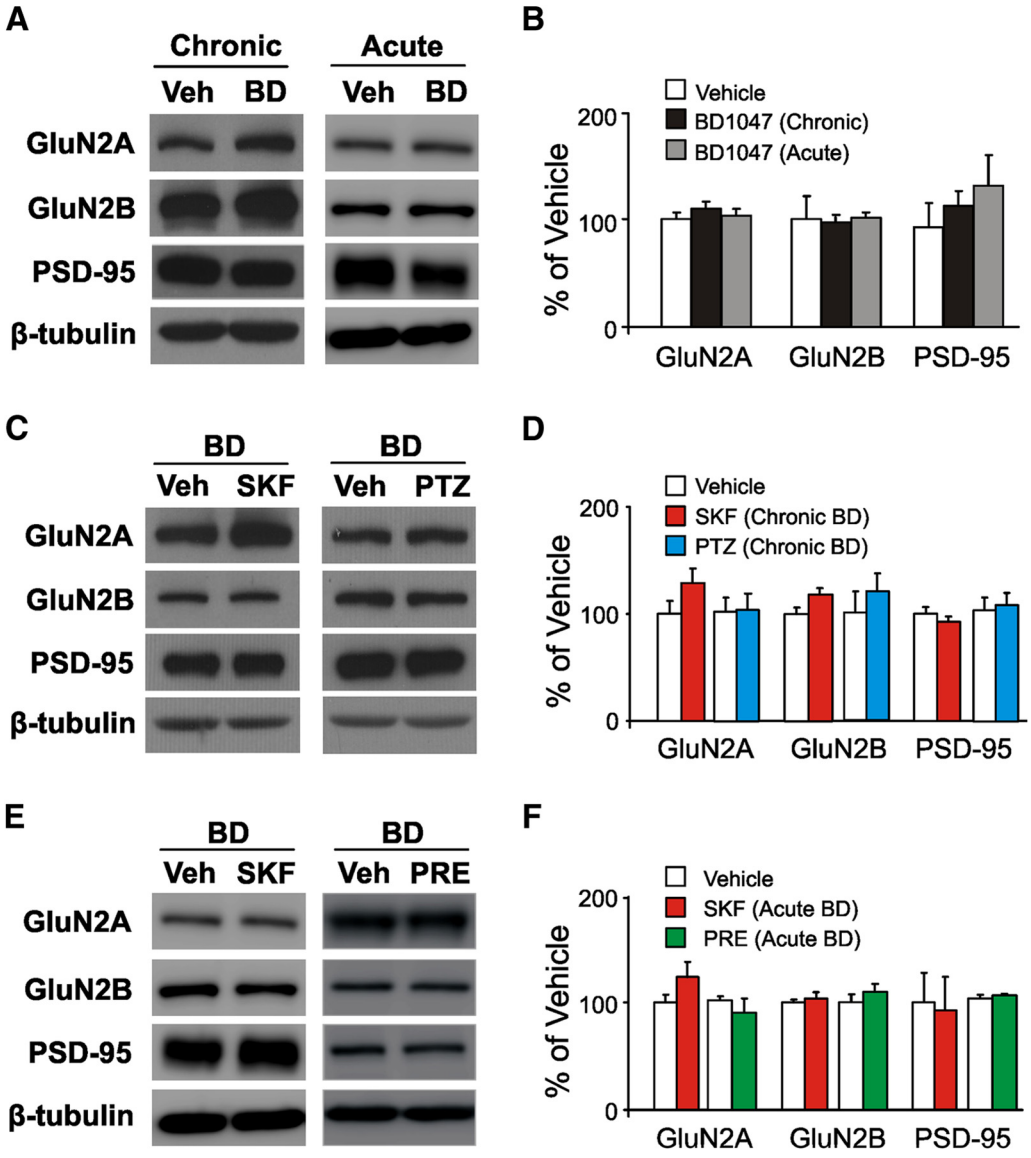

Figure 4. Chronic and acute administration of BD1047 abolishes the σ-1R-mediated increase in NMDAR subunit and PSD-95 expression *in vivo*. ***A***, ***B***, There was no change in the expression level of GluN2A, GluN2B, or PSD-95 after a 2 d chronic administration or a single intraperitoneal injection (acute administration) of vehicle (Veh) or the σ-1R antagonist BD1047 (BD). ***C***, ***D***, Chronic administration of BD1047 blocked the increase in GluN2 subunit and PSD-95 levels observed 90 min after an intraperitoneal injection of SKF or PTZ. ***E***, ***F***, Acute administration of BD1047 also abolished the increase in GluN2 subunits and PSD-95 expression after administration of SKF or PRE. Bar graphs are mean ± SEM of at least five animals.

$p = 0.77$; PSD-95, 93 ± 5.8% of vehicle, $p = 0.31$, $n = 5$). Likewise, the expression levels were not altered after a single, acute intraperitoneal injection of BD1047 (Fig. 4*A*,*B*, Table 2); expression levels of GluN2A (126 ± 11% of vehicle, $p = 0.27$, $n = 3$), GluN2B (104 ± 3.3% of vehicle, $p = 0.64$, $n = 3$), or PSD-95 (124 ± 44% of vehicle, $p = 0.65$, $n = 3$) were unaffected after a single intraperitoneal injection of BD1047 (Fig. 4*B*).

Chronic administration of BD1047 prevented the robust increase in GluN2 subunits and PSD-95 observed 90 min after SKF administration (Fig. 4*C*,*D*, Table 2: GluN2A, 128 ± 14%, $p = 0.33$; GluN2B, 118 ± 6.5%, $p = 0.23$, $n = 5$; PSD-95, 78 ± 14% of vehicle, $p = 0.55$, $n = 3$). When the experiment was repeated using PTZ, the expression levels of GluN2 subunits and PSD-95 were not significantly changed after chronic BD1047 administration (Fig. 4*C*,*D*, Table 2: GluN2A, 101 ± 14%, $p = 0.76$; GluN2B, 118 ± 16%, $p = 0.64$; PSD-95, 105 ± 2.1% of vehicle, $p = 0.31$, $n = 5$). There was also no significant change in GluN2 subunit and PSD-95 expression levels when SKF was injected 1 h after acute administration of BD1047 (Fig. 4*E*,*F*, Table 2: GluN2A, 114 ± 7.8, $p = 0.27$; GluN2B, 104 ± 9.6%, $p = 0.69$; PSD-95, 71 ± 14% of vehicle, $p = 0.43$, $n = 3$). Similar results were obtained when PRE was administered 1 h after σ-1R antagonist treatment (Fig. 4*E*,*F*, Table 2: GluN2A, 94 ± 4.8%, $p = 0.60$; GluN2B, 111 ± 8.9%, $p = 0.34$; PSD-95, 105 ± 0.75% of vehicle, $p = 0.10$, $n = 3$). Thus, these experiments demonstrate that both chronic and acute administration of one of two σ-1R antagonists are able to block the upregulation of GluN2 subunits and PSD-95 observed after injection of any one of the three σ-1R agonists under study (Table 2). Together, our pharmacological experiments show that activation of σ-1Rs is mediating an increase in GluN2 and PSD-95 levels in the rat hippocampus.

The σ-1R-mediated increase in GluN2 subunit and PSD-95 expression is protein synthesis dependent

Recent studies have shown that σ-1R activation regulates protein expression of a number of membrane-bound ion channels

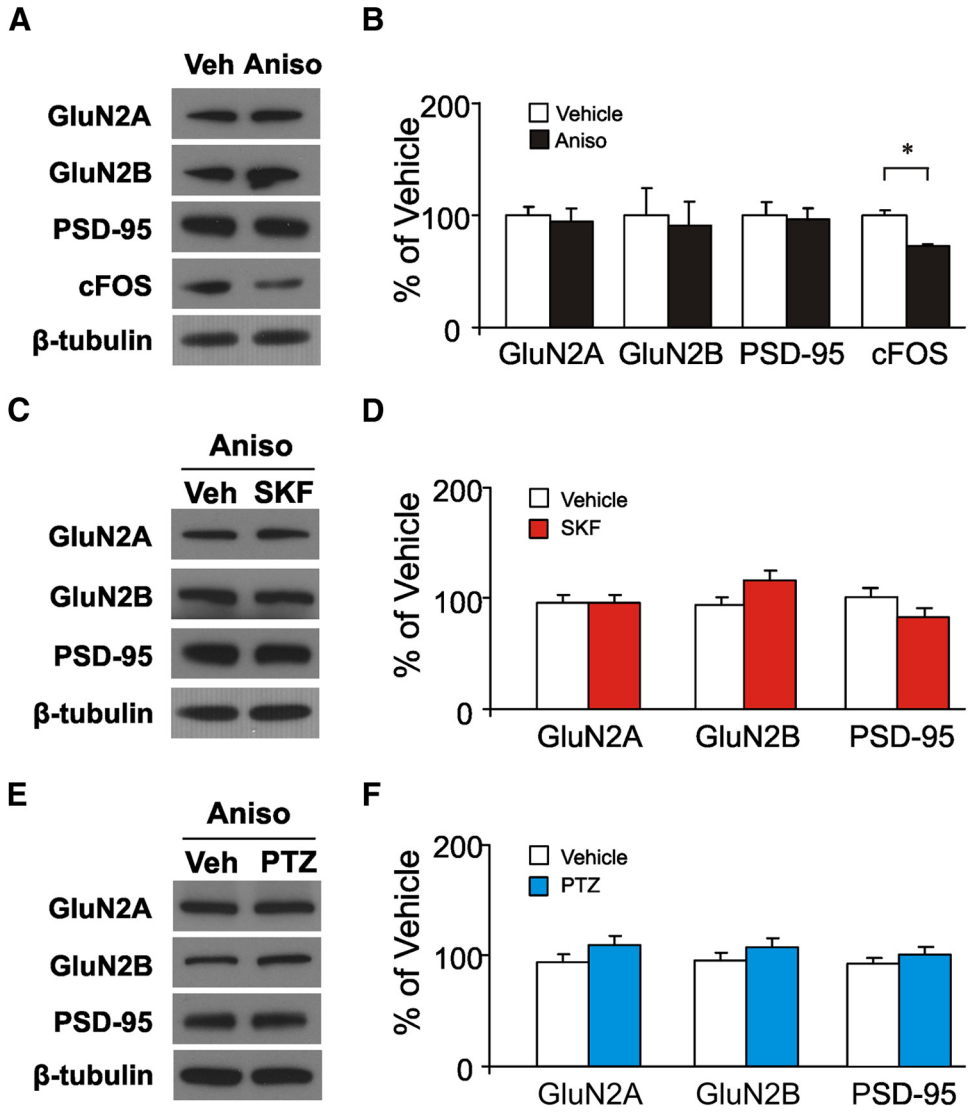

Figure 5. The increase in GluN2 subunits and PSD-95 expression after σ-1R activation is protein synthesis dependent. ***A***, Representative WBs showing that the expression levels of GluN2A, GluN2B, and PSD-95 were unaffected by intraperitoneal injection of vehicle (Veh) or anisomycin (Aniso). However, there was a decrease in the expression level of c-Fos (***B***), demonstrating that anisomycin blocked protein synthesis at this time point. Interestingly, anisomycin treatment before SKF (***C***, ***D***) or PTZ (***E***, ***F***) administration prevented any change in expression levels of GluN2 subunits and PSD-95. Bar graphs are mean ± SEM of at least five animals. $*p < 0.05$.

(Ishima et al., 2008; Nishimura et al., 2008; Crottès et al., 2011). Therefore, the increase in GluN2 subunit and PSD-95 expression after σ-1R agonist administration could arise from *de novo* protein synthesis. In this case, inhibiting protein synthesis should abolish the upregulation of GluN2 subunits and PSD-95 observed after injection of σ-1R agonists. To test this hypothesis, the protein synthesis inhibitor anisomycin (Wanisch and Wotjak, 2008) was administered 1 h before challenging the animals with σ-1R agonists. To validate that anisomycin effectively blocked protein synthesis in our experimental paradigm, we monitored c-Fos levels, a commonly used marker for protein synthesis (Fischer et al., 2004). Expression of c-Fos was significantly reduced (Fig. 5*A*,*B*: 73 ± 1% of vehicle, $p < 0.05$, $n = 4$) after anisomycin administration (30 mg/kg) alone when compared with vehicle, indicating a decrease in *de novo* protein synthesis. In addition, anisomycin did not alter GluN2 subunit or PSD-95 expression (Fig. 5*A*,*B*: GluN2A, 94 ± 4.4%, $p = 0.26$; GluN2B, 90 ± 15%, $p = 0.78$; PSD-95, 88 ± 4.7% of vehicle, $p = 0.42$, $n = 4$). However, anisomycin pretreatment abolished the SKF-mediated increase in GluN2 subunit and PSD-95 expression (Fig. 5*C*,*D*: GluN2A, 102 ± 7%, $p = 0.86$; GluN2B, 116 ± 8%, $p = 0.20$; PSD-95, 87 ± 7.6% of vehicle, $p = 0.52$, $n = 5$). Similar results were obtained when PTZ was administered after anisomycin treatment (Fig. 5*E*,*F*: GluN2A, 118 ± 8%, $p = 0.28$; GluN2B, 115 ± 16%, $p = 0.61$; PSD-95, 111 ± 3.8% of vehicle, $p = 0.28$, $n = 6$). These results demonstrate that the increase in GluN2 subunits and PSD-95 is dependent on *de novo* protein synthesis. Therefore, we show that the σ-1R activation leads to an increase in GluN2 subunits and PSD-95 by increasing protein synthesis.

Increased interaction between σ-1Rs and NMDARs after σ-1R activation

One well established role of σ-1Rs is as ligand-activated scaffolds to assist in protein trafficking (Su et al., 2010). Therefore, we speculated that, during activation, σ-1Rs may associate with NMDAR/PSD-95 complexes, followed by trafficking to the plasma membrane. To investigate this possibility, we performed Co-IP experiments 90 min after SKF or vehicle injection. We

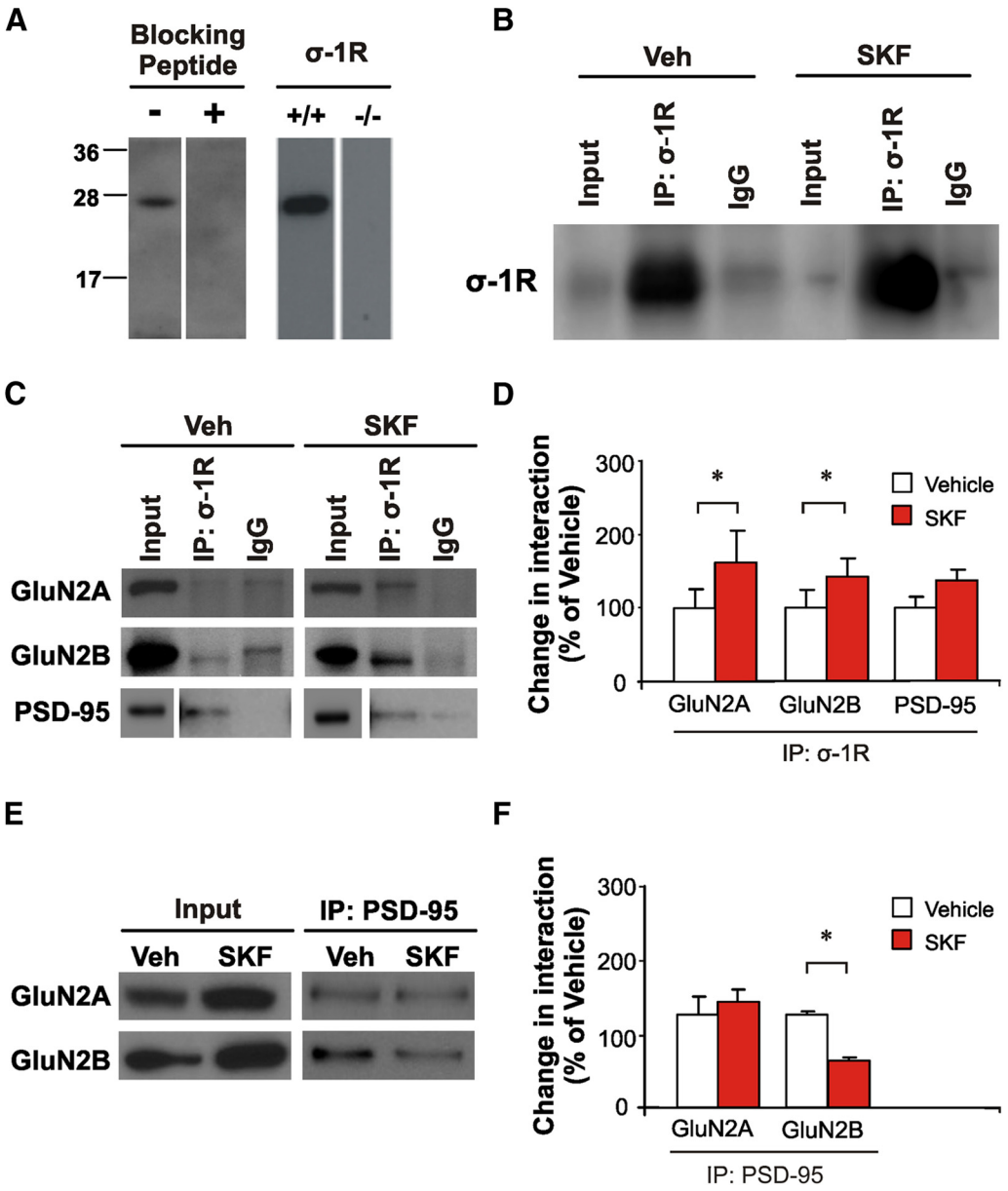

Figure 6. An increase in interaction between σ-1Rs and NMDARs was observed after SKF injection. ***A***, Representative blots showing the specificity of the σ-1R antibody. Single σ-1Rs band detected in rat brain homogenate was abolished in the presence of blocking peptide (***A***, left). Similarly, the single σ-1Rs band in wild-type mouse hippocampus was not detected in σ-1R $^{-/-}$ mice (***A***, right). ***B***, Control Co-IP experiment demonstrating that σ-1Rs were immunoprecipitated and detected with the σ-1R antibody. ***C***, Representative WBs from a Co-IP experiment investigating the interaction between σ-1Rs and GluN2 subunits, demonstrating an increased interaction after SKF administration compared with vehicle (Veh). ***D***, Pooled data showing a significant increase in interaction between σ-1Rs and GluN2 subunits after SKF injection. ***E***, Representative WBs from an additional experiment investigating the interaction between PSD-95 and GluN2 subunits after SKF administration. ***F***, The binding of PSD-95 with GluN2A was unaffected by SKF; interestingly, a significant decrease in the interaction between PSD-95 and GluN2B was observed. Bar graphs are mean ± SEM of at least five animals. *$p < 0.05$.

chose to focus on SKF in all subsequent experiments because of the robust response observed after its administration (Fig. 2*A*,*B*).

To ensure the specificity of the σ-1R antibody, we performed WB experiments on rat LP1 samples in the presence and absence of σ-1R blocking peptide (Fig. 6*A*, left), as well as on hippocampi obtained from wild-type and σ-1R $^{-/-}$ mice (Fig. 6*A*, right). When the WBs were probed for σ-1Rs without blocking peptide in rats or wild-type mice, a single band at ~29 kDa was observed, which corresponds to σ-1Rs. This band was absent in the presence of σ-1R blocking peptide and in LP1 extracts obtained from σ-1R $^{-/-}$ mice. We also verified our Co-IP protocol by immunoprecipitating with σ-1Rs and detecting with σ-1Rs after vehicle or SKF administration (Fig. 6*B*). A single band was observed in both vehicle and SKF treatment with little nonspecific binding (IgG). Thus, our control experiments show that we were able to immunoprecipitate σ-1Rs with the antibody used.

To investigate whether activation of σ-1Rs influenced the binding to NMDAR and PSD-95, we immunoprecipitated σ-1R, followed by WB for GluN2A, GluN2B, and PSD-95. In all of our Co-IP experiments, there was either a very weak or no interaction between the control IgG and any of the proteins under study (Fig. 6*C*). After SKF administration, there was an increased interaction of GluN2A and GluN2B with σ-1Rs (Fig. 6*C*,*D*: GluN2A, 163 ± 24%; GluN2B, 142 ± 10% of vehicle, $p < 0.05$, $n = 4$) but not with PSD-95 (137 ± 14%, $p = 0.32$, $n = 4$). When the reverse experiment was performed (IP with GluN2A, GluN2B, or

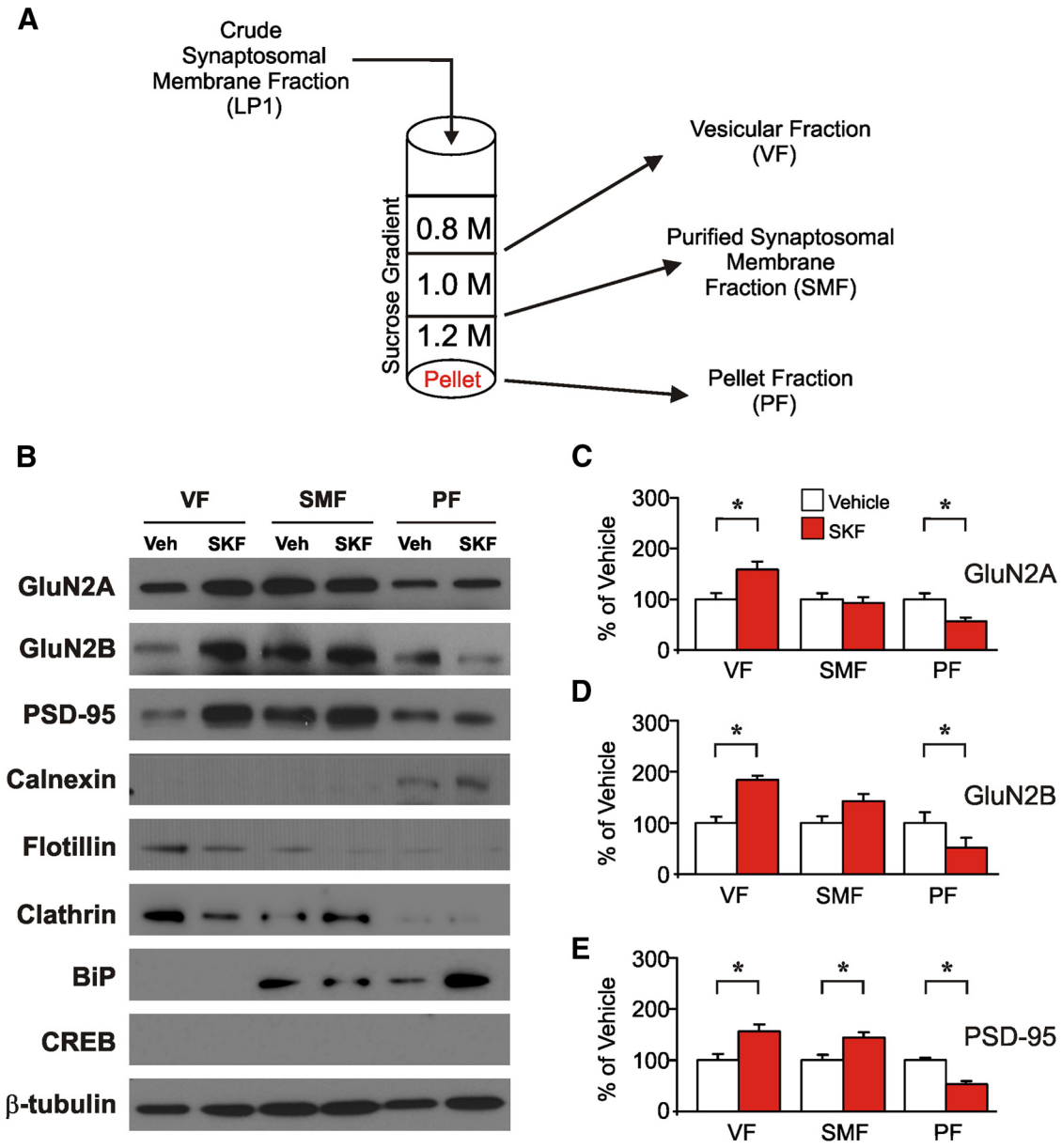

Figure 7. A redistribution of GluN2 subunits and PSD-95 was observed after administration of SKF. ***A***, Schematic diagram showing the three fractions isolated from LP1 by discontinuous sucrose gradient. ***B***, Representative WBs showing protein expression in the different fractions after injection of vehicle (Veh) or SKF with β-tubulin as a loading control. A significant increase in GluN2A (***C***) and GluN2B (***D***) expression was observed in the VF and a significant increase in PSD-95 (***E***) in both VF and SMF after SKF administration. There is a decrease in expression in the PF for all three proteins investigated (***C–E***). Bar graphs are mean ± SEM of at least four animals. *$p < 0.05$.

PSD-95 and WB for σ-1Rs), we also observed an increased interaction of GluN2 subunits with σ-1Rs (GluN2A, 152 ± 6.9%; GluN2B, 197 ± 14% of vehicle, $p < 0.05$, $n = 3$) but not with PSD-95 (99 ± 16%, $p = 0.96$, $n = 3$) after σ-1R activation.

Because PSD-95 binds directly to GluN2 subunits (Kornau et al., 1995), we investigated whether the increased interaction observed between σ-1Rs and GluN2 subunits after SKF administration could affect PSD-95 binding to GluN2 subunits. To do this, we immunoprecipitated PSD-95 and probed with antibodies against the GluN2 subunits after administration of vehicle or SKF. No change could be detected in the interaction between PSD-95 and GluN2A after SKF administration (Fig. 6*E*,*F*: 114 ± 18% of vehicle, $p = 0.74$, $n = 4$), suggesting that binding of σ-1Rs to GluN2A occurs without affecting the binding of PSD-95 to GluN2A. However, a significant decrease in the amount of GluN2B bound to PSD-95 was observed after SKF administration (Fig. 6*F*: 50 ± 4.1% of vehicle, $p < 0.05$, $n = 4$). Together, our Co-IP experiments indicate that there is an increased complex formation between GluN2 subunits and σ-1Rs after SKF administration and that σ-1R activation disrupts the association between GluN2B and PSD-95.

σ-1R activation leads to the redistribution of GluN2A, GluN2B, and PSD-95 between intracellular compartments

Because σ-1Rs are involved in translocation of proteins (Morin-Surun et al., 1999; Kourrich et al., 2013), they may facilitate transport of NMDARs to the plasma membrane. Thus, we would expect an increase in GluN2 subunit expression in transport vesicles and/or postsynaptic membranes after SKF administration.

To test this hypothesis, three-step discontinuous sucrose gradient centrifugation experiments were performed on LP1 fractions to elucidate the subcellular localization and move-

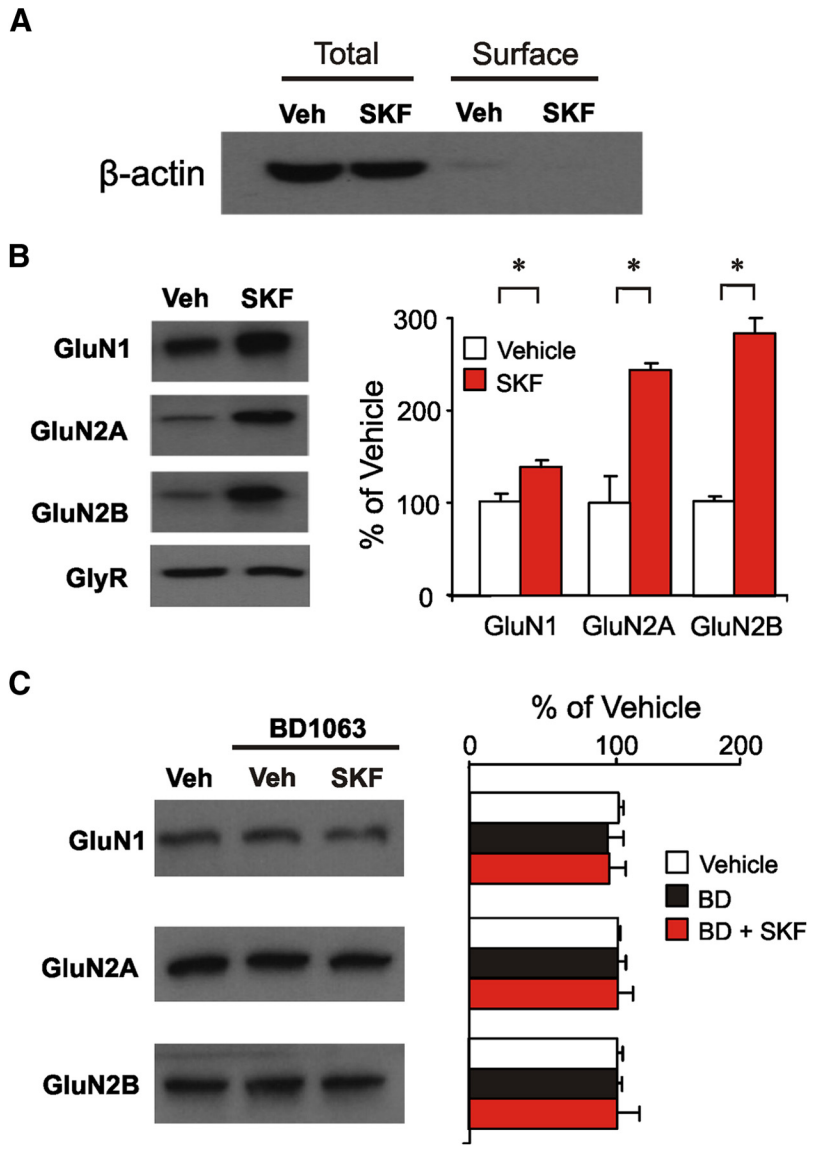

Figure 8. An increase in surface levels of NMDARs was observed after administration of SKF. ***A***, Representative WB of β-actin in the whole homogenate (Total) and the biotinylated (Surface) fractions showing a marked reduction in band intensity in the surface fraction, typical of an intracellular protein. ***B***, There was an upregulation in surface levels of NMDAR subunits after SKF injection compared with vehicle (Veh). ***C***, This effect was blocked after pretreatment with the σ-1R antagonist BD1063 (BD). Bar graphs are mean ± SEM of at least five animals. *$p < 0.05$.

ment of GluN2 subunits and PSD-95 after σ-1R activation (Fig. 7*A*). The VF is enriched at the 0.8 and 1.0 M sucrose interface and contains transporter vesicles, whereas the SMF is enriched at the 1.0 and 1.2 M sucrose interface and contains synaptic membranes. The PF contains intracellular organelles, such as ER and mitochondria (Blackstone et al., 1992). To verify the purity of our fractions, we probed for proteins that act as markers for particular fractions. Figure 7*B* shows that flotillin was enriched in VF and SMF fractions (Nebl et al., 2002), whereas calnexin was only present in the PF as expected (Villa et al., 1992). Clathrin was enriched in VF and SMF but not PF (Fig. 7*B*), again expected given its role in receptor endocytosis (Sato et al., 1995). In contrast, the ER-resident protein BiP was not present in the VF (Fig. 7*B*) but was present in the SMF and PF (Gardner et al., 2013). The nuclear resident protein CREB (Platenik et al., 2005) was not detected in any of our sucrose gradient fractions (Fig. 7*B*).

After SKF administration, GluN2A and GluN2B protein levels were significantly enhanced in VF (Fig. 7*C*,*D*: GluN2A, 162 ± 24%; GluN2B, 174 ± 13% of vehicle, $p < 0.05$, $n = 5$) but were unaltered in SMF after SKF administration (GluN2A, 97 ± 11%, $p = 0.94$; GluN2B, 120 ± 9.0% of vehicle, $p = 0.25$, $n = 5$). The levels of PSD-95 were significantly increased in both VF and SMF (Fig. 7*E*: 156.5 ± 12% and 143 ± 10% of vehicle respectively, $p < 0.05$, $n = 5$). Furthermore, there was a significant decrease in the levels of all three proteins in the PF after SKF administration (Fig. 7*C–E*: GluN2A, 78 ± 11%; GluN2B, 51 ± 19%; PSD-95, 52 ± 6.8% of vehicle, $p < 0.05$, $n = 5$), suggesting that there is movement of these proteins out of subcellular organelles. Thus, σ-1R activation leads to an increase in GluN2A, GluN2B, and PSD-95 protein levels in vesicles, along with an increase in PSD-95 in the SMF. This increase is likely attributable to an enhanced export of newly synthesized proteins after SKF treatment, although possible contributions from degradation or endocytotic vesicles cannot be ruled out.

σ-1R activation leads to an increase in surface levels of NMDARs

Thus far, we have demonstrated that σ-1R activation leads to increased protein synthesis and trafficking of GluN2 subunits. One obvious question is whether these subunits can be inserted in the plasma membrane, thereby resulting in an increase in NMDAR surface expression. To address this, we performed surface biotinylation experiments after an intraperitoneal injection of vehicle or SKF. Figure 8*A* shows a representative blot of β-actin intensity in total and surface fractions after vehicle or SKF injection, demonstrating that our protocol enables us to detect changes in surface protein levels with no significant contamination from intracellular proteins (e.g., β-actin). We also probed for GlyRs and observed no change in surface levels after SKF administration (Fig. 8*B*). A significant increase in surface GluN2A (242 ± 20% of vehicle, $p < 0.05$, $n = 3$) and GluN2B (289 ± 21% of vehicle, $p < 0.05$, $n = 3$) subunit expression could be detected after injection of SKF (Fig. 8*B*). Interestingly, the levels of surface GluN1 subunits also increased after σ-1R activation (129 ± 3.8% of vehicle, $p < 0.05$, $n = 3$). As a control, the surface expression levels of AMPARs showed no change after SKF treatment (GluA1, 125 ± 14%, $p = 0.30$; GluA2, 116 ± 15%, $p = 0.42$; GluA2/3/4, 117 ± 19% of vehicle, $p = 0.27$, $n = 8$).

To demonstrate that this effect was mediated via σ-1R activation, we repeated the experiments in the presence of a σ-1R antagonist. Chronic administration of BD1063 had no effect on NMDAR subunit surface expression in and of itself (Fig. 8*C*: GluN1, 93 ± 11%, $p = 0.86$; GluN2A, 98.5 ± 3.47%, $p = 0.33$;

GluN2B, 98 ± 2.7%, $p = 0.09$ of vehicle $n = 4$). Administration of BD1063 completely abolished the SKF-induced increase in surface expression of NMDAR subunits (Fig. 8*C*: GluN1, 95 ± 11.4%, $p = 0.64$; GluN2A, 103 ± 11.2%, $p = 0.55$; GluN2B, 106 ± 15.3% of vehicle, $p = 0.90$, $n = 4$). As expected, there was no effect on the surface expression of GluA1 subunit with BD1063 alone (98 ± 8.7% of vehicle, $p = 0.68$, $n = 4$) or in combination with SKF (106 ± 11% of vehicle, $p = 0.72$, $n = 4$). This shows that activation of σ-1Rs leads to an insertion of NMDARs in the plasma membrane.

Discussion

The data presented in this study (summarized in Fig. 9) demonstrate that σ-1R activation leads to an increase in *de novo* protein synthesis of GluN2A, GluN2B, and PSD-95 (Figs. 1–5). After σ-1R activation, we also observe an enhanced interaction between σ-1Rs and NMDARs (Fig. 6) and an intracellular redistribution of GluN2 subunits and PSD-95 (Fig. 7). In addition, activation of σ-1Rs leads to a increase in NMDARs at the plasma membrane (Fig. 8). These results provide insight into how σ-1Rs may influence NMDAR expression and trafficking in hippocampal neurons.

Interestingly, σ-1R activation did not alter the expression level of GluN1 subunits (Fig. 2). One explanation for this is that the availability of GluN2 subunits may be the limiting factor for the assembly of stable NMDARs and that GluN1 subunit expression is regulated by different mechanisms. In agreement with this hypothesis, previous work in cultured neurons reveals that the majority of GluN1 subunits reside in an intracellular pool with rapid turnover and that this pool is not associated with GluN2 subunits (Huh and Wenthold, 1999). When GluN1 subunits associate with GluN2 subunits, the resulting complex is efficiently trafficked to the plasma membrane (McIlhinney et al., 1996; Huh and Wenthold, 1999).

Because σ-1Rs have a well established role as an inter-organelle signaling modulator (Su et al., 2010), they may aid trafficking of NMDARs to the plasma membrane. A prediction arising from this hypothesis is that σ-1Rs and NMDARs may form a macromolecular complex and that σ-1R agonists should be able to modulate this interaction. Indeed, the results obtained from our Co-IP experiments reveal that there is an interaction between σ-1Rs and the GluN2 subunits, which is enhanced after σ-1R activation (Fig. 6). Direct interactions between σ-1Rs and NMDARs have also been observed in a recombinant system (Balasuriya et al., 2013). However, there appears to be a discrepancy with regards to the locus of σ-1R binding. Our data suggest that σ-1Rs bind directly to GluN2 subunits (Fig. 6), whereas direct binding of σ-1Rs to GluN1 subunits is observed in recombinant cells (Balasuriya et al., 2013). Because it is well established that NMDARs are tetramers composed of two GluN1 and two GluN2 subunits with a 1–2-1–2 stoichiometry (Salussolia et al., 2011; Karakas and Furukawa, 2014; Lee et al., 2014), we cannot rule out the possibility that, in our Co-IP experiments, σ-1Rs are directly binding to the GluN1 subunit and we are detecting this interaction when probing for GluN2 subunits.

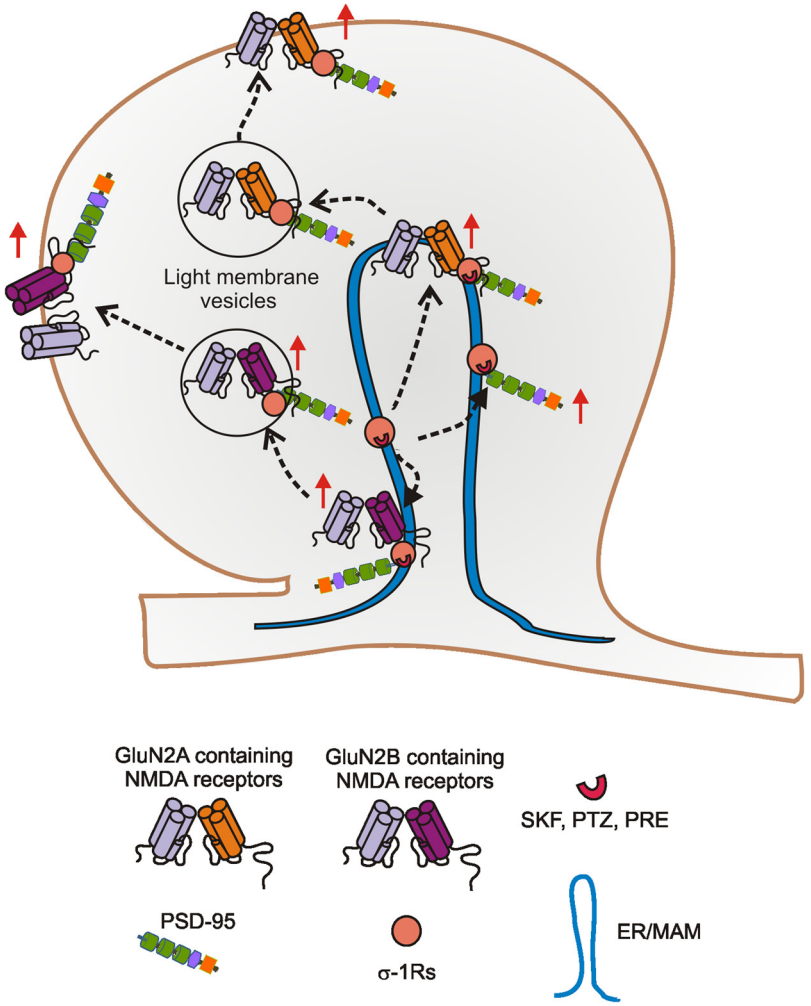

Figure 9. Proposed model of NMDAR modulation after σ-1R activation. Schematic diagram showing a proposed mechanism by which activation of σ-1Rs leads to an increase in plasma membrane NMDARs. Solid red arrows represent an increase in NMDAR expression, and the dashed arrows represent potential trafficking events.

One intriguing result from our Co-IP experiments was a decrease in interaction between GluN2B and PSD-95 after σ-1R activation (Fig. 6*E*,*F*). Because GluN2A and GluN2B have preferred associations with PSD-95 and synapse-associated protein 102 (SAP102), respectively (Sans et al., 2000), we speculate that σ-1Rs may further segregate these subunits during trafficking. Because PSD-95 is preferentially expressed at the postsynaptic density whereas SAP102 is more evenly distributed (for review, see Sanz-Clemente et al., 2013), disruption of the GluN2B/PSD-95 association after σ-1R activation may promote preferential trafficking of GluN2B-containing NMDARs to extrasynaptic sites.

Previous work suggests that σ-1Rs interact with ligand-gated ion channels before exiting the Golgi (Crottès et al., 2011; Balasuriya et al., 2013). Because σ-1Rs are located at the interface between the ER and the mitochondria-associated ER membrane (MAM; Hayashi and Su, 2007), the obvious locus of interaction between σ-1Rs and NMDARs could be at the ER or Golgi. If σ-1Rs are acting as trafficking scaffolds to facilitate export of NMDARs, we hypothesize that a redistribution of NMDARs

should be observed after σ-1R activation. To reflect movement of NMDARs from the ER to the plasma membrane, we would expect to observe a decrease in the NMDAR content of the PF, along with a concomitant increase in the VF and/or SMF. Consistent with this hypothesis, there is a decrease in protein expression in PF for both GluN2 subunits and PSD-95 after SKF administration (Fig. 7), suggesting that σ-1Rs could act as a scaffold in transport out of the ER/MAM compartment (Hayashi and Su, 2007; Kourrich et al., 2013).

As expected, GluN2A, GluN2B, and PSD-95 were all significantly increased in VF after SKF injection (Fig. 7). Previous reports have demonstrated that the GluN2B subunit is transported in exocytotic vesicles as large protein complexes containing PSD-95 (Guillaud et al., 2003; Standley et al., 2012). This suggests that the increase in VF may reflect an increase in GluN2 subunit and PSD-95 trafficking to the plasma membrane. Studies showing sorting of σ-1Rs to exocytotic vesicles after administration of σ-1R agonists (Hayashi and Su, 2003; Kourrich et al., 2012) provide some evidence to support this hypothesis. However, an increase in VF could also be attributable to an increase in vesicles containing GluN2 subunits/PSD-95 for recycling. In this regard, additional experiments are required to fully resolve the subcellular dynamics of GluN2 subunits after σ-1R activation.

The σ-1R-mediated increase in NMDAR levels at the plasma membrane that we observe (Fig. 8) may have wide-ranging functional consequences given that NMDARs are implicated in an array of physiological (e.g., synaptic plasticity) and pathological (e.g., excitotoxicity) functions. Further understanding the relationship between σ-1R activation and NMDAR physiology will provide exciting new avenues for therapeutics in an array of CNS disorders.

References

Aydar E, Palmer CP, Klyachko VA, Jackson MB (2002) The sigma receptor as a ligand-regulated auxiliary potassium channel subunit. Neuron 34: 399–410. CrossRef Medline

Balasuriya D, Stewart AP, Edwardson JM (2013) The sigma-1 receptor interacts directly with GluN1 but not GluN2A in the GluN1/GluN2A NMDA receptor. J Neurosci 33:18219–18224. CrossRef Medline

Bergeron R, de Montigny C, Debonnel G (1995) Biphasic effects of sigma ligands on the neuronal response to *N*-methyl-D-aspartate. Naunyn Schmiedebergs Arch Pharmacol 351:252–260. Medline

Bergeron R, de Montigny C, Debonnel G (1996) Potentiation of neuronal NMDA response induced by dehydroepiandrosterone and its suppression by progesterone: effects mediated via sigma receptors. J Neurosci 16: 1193–1202. Medline

Bergeron R, de Montigny C, Debonnel G (1997) Effect of short-term and long-term treatments with sigma ligands on the *N*-methyl-D-aspartate response in the CA3 region of the rat dorsal hippocampus. Br J Pharmacol 120:1351–1359. CrossRef Medline

Beskid M, Rózycka Z, Taraszewska A (1998) Quinolinic acid and sigma receptor ligand: effect on pyramidal neurons of the CA1 sector of dorsal hippocampus following peripheral administration in rats. Folia Neuropathol 36:94–100. Medline

Blackstone CD, Moss SJ, Martin LJ, Levey AI, Price DL, Huganir RL (1992) Biochemical characterization and localization of a non-*N*-methyl-D-aspartate glutamate receptor in rat brain. J Neurochem 58:1118–1126. CrossRef Medline

Crottès D, Martial S, Rapetti-Mauss R, Pisani DF, Loriol C, Pellissier B, Martin P, Chevet E, Borgese F, Soriani O (2011) Sig1R protein regulates hERG channel expression through a post-translational mechanism in leukemic cells. J Biol Chem 286:27947–27958. CrossRef Medline

Debonnel G, Bergeron R, de Montigny C (1996a) Potentiation by dehydroepiandrosterone of the neuronal response to *N*-methyl-D-aspartate in the CA3 region of the rat dorsal hippocampus: an effect mediated via sigma receptors. J Endocrinol [Suppl] 150:S33–S42.

Debonnel G, Bergeron R, Monnet FP, De Montigny C (1996b) Differential effects of sigma ligands on the *N*-methyl-D-aspartate response in the CA1 and CA3 regions of the dorsal hippocampus: effect of mossy fiber lesioning. Neuroscience 71:977–987. CrossRef Medline

de Montigny C, Monnet FP, Fournier A, Debonnel G (1992) Sigma ligands and neuropeptide Y selectively potentiate the NMDA response in the rat CA3 dorsal hippocampus: in vivo electrophysiological studies. Clin Neuropharmacol 15 [Suppl 1]:145A–146A.

Dennis SH, Jaafari N, Cimarosti H, Hanley JG, Henley JM, Mellor JR (2011) Oxygen/glucose deprivation induces a reduction in synaptic AMPA receptors on hippocampal CA3 neurons mediated by mGluR1 and adenosine A3 receptors. J Neurosci 31:11941–11952. CrossRef Medline

Fischer A, Sananbenesi F, Schrick C, Spiess J, Radulovic J (2004) Distinct roles of hippocampal de novo protein synthesis and actin rearrangement in extinction of contextual fear. J Neurosci 24:1962–1966. CrossRef Medline

Fischer von Mollard G, Stahl B, Walch-Solimena C, Takei K, Daniels L, Khoklatchev A, De Camilli P, Südhof TC, Jahn R (1994) Localization of Rab5 to synaptic vesicles identifies endosomal intermediate in synaptic vesicle recycling pathway. Eur J Cell Biol 65:319–326. Medline

Fletcher EJ, Church J, Abdel-Hamid K, MacDonald JF (1995) Blockade by sigma site ligands of *N*-methyl-D-aspartate-evoked responses in rat and mouse cultured hippocampal pyramidal neurones. Br J Pharmacol 116: 2791–2800. CrossRef Medline

Forder JP, Tymianski M (2009) Postsynaptic mechanisms of excitotoxicity: Involvement of postsynaptic density proteins, radicals, and oxidant molecules. Neuroscience 158:293–300. CrossRef Medline

Gardner BM, Pincus D, Gotthardt K, Gallagher CM, Walter P (2013) Endoplasmic reticulum stress sensing in the unfolded protein response. Cold Spring Harb Perspect Biol 5:a013169. CrossRef Medline

Guillaud L, Setou M, Hirokawa N (2003) KIF17 dynamics and regulation of NR2B trafficking in hippocampal neurons. J Neurosci 23:131–140. Medline

Gundlach AL, Largent BL, Snyder SH (1986) Autoradiographic localization of sigma receptor binding sites in guinea pig and rat central nervous system with (+)3H-3-(3-hydroxyphenyl)-N-(1-propyl)piperidine. J Neurosci 6:1757–1770. Medline

Hallett PJ, Collins TL, Standaert DG, Anthone W (2008) Biochemical fractionation of brain tissue for studies of receptor distribution and trafficking. Curr Protoc Neurosci Chapter 1:Unit 1.16. CrossRef

Hayashi T, Su TP (2003) Intracellular dynamics of sigma-1 receptors (sigma-1 binding sites) in NG108–15 cells. J Pharmacol Exp Ther 306: 726–733. CrossRef Medline

Hayashi T, Su TP (2007) Sigma-1 receptor chaperones at the ER-mitochondrion interface regulate Ca(2+) signaling and cell survival. Cell 131:596–610. CrossRef Medline

Huh KH, Wenthold RJ (1999) Turnover analysis of glutamate receptors identifies a rapidly degraded pool of the *N*-methyl-D-aspartate receptor subunit, NR1, in cultured cerebellar granule cells. J Biol Chem 274:151–157. CrossRef Medline

Ishima T, Nishimura T, Iyo M, Hashimoto K (2008) Potentiation of nerve growth factor-induced neurite outgrowth in PC12 cells by donepezil: role of sigma-1 receptors and IP3 receptors. Prog Neuropsychopharmacol Biol Psychiatry 32:1656–1659. CrossRef Medline

Johannessen M, Ramachandran S, Riemer L, Ramos-Serrano A, Ruoho AE, Jackson MB (2009) Voltage-gated sodium channel modulation by sigma-receptors in cardiac myocytes and heterologous systems. Am J Physiol Cell Physiol 296:C1049–C1057. CrossRef Medline

Karakas E, Furukawa H (2014) Crystal structure of a heterotetrameric NMDA receptor ion channel. Science 344:992–997. CrossRef Medline

Kerchner GA, Nicoll RA (2008) Silent synapses and the emergence of a postsynaptic mechanism for LTP. Nat Rev Neurosci 9:813–825. CrossRef Medline

Kinoshita M, Matsuoka Y, Suzuki T, Mirrielees J, Yang J (2012) Sigma-1 receptor alters the kinetics of Kv1.3 voltage gated potassium channels but not the sensitivity to receptor ligands. Brain Res 1452:1–9. CrossRef Medline

Kornau HC, Schenker LT, Kennedy MB, Seeburg PH (1995) Domain interaction between NMDA receptor subunits and the postsynaptic density protein PSD-95. Science 269:1737–1740. CrossRef Medline

Kourrich S, Su TP, Fujimoto M, Bonci A (2012) The sigma-1 receptor: roles in neuronal plasticity and disease. Trends Neurosci 35:762–771. CrossRef Medline

Kourrich S, Hayashi T, Chuang JY, Tsai SY, Su TP, Bonci A (2013) Dynamic interaction between sigma-1 receptor and Kv1.2 shapes neuronal and behavioral responses to cocaine. Cell 152:236–247. CrossRef Medline

Langa F, Codony X, Tovar V, Lavado A, Giménez E, Cozar P, Cantero M, Dordal A, Hernández E, Pérez R, Monroy X, Zamanillo D, Guitart X, Montoliu L (2003)

Generation and phenotypic analysis of sigma receptor type I (sigma 1) knockout mice. Eur J Neurosci 18:2188–2196. CrossRef Medline

Lee CH, Lü W, Michel JC, Goehring A, Du J, Song X, Gouaux E (2014) NMDA receptor structures reveal subunit arrangement and pore architecture. Nature 511:191–197. CrossRef Medline

Lupardus PJ, Wilke RA, Aydar E, Palmer CP, Chen Y, Ruoho AE, Jackson MB (2000) Membrane-delimited coupling between sigma receptors and K+ channels in rat neurohypophysial terminals requires neither G-protein nor ATP. J Physiol 526:527–539. CrossRef Medline

Martina M, Turcotte ME, Halman S, Bergeron R (2007) The sigma-1 receptor modulates NMDA receptor synaptic transmission and plasticity via SK channels in rat hippocampus. J Physiol 578:143–157. Medline

Matsumoto RR (2007) Sigma receptors: historical perspective and background, Chap 1. In: Sigma receptors chemistry, cell biology and clinical implications (Matsumoto RR, Bowen WD, Su TP, eds), pp 125. New York: Springer Science + Business Media.

Matsumoto RR, Bowen WD, Tom MA, Vo VN, Truong DD, De Costa BR (1995) Characterization of two novel sigma receptor ligands: antidystonic effects in rats suggest sigma receptor antagonism. Eur J Pharmacol 280:301–310. CrossRef Medline

Maurice T, Su TP (2009) The pharmacology of sigma-1 receptors. Pharmacol Ther 124:195–206. CrossRef Medline

McCracken KA, Bowen WD, de Costa BR, Matsumoto RR (1999) Two novel sigma receptor ligands, BD1047 and LR172, attenuate cocaine-induced toxicity and locomotor activity. Eur J Pharmacol 370:225–232. CrossRef Medline

McIlhinney RA, Molnár E, Atack JR, Whiting PJ (1996) Cell surface expression of the human *N*-methyl-D-aspartate receptor subunit 1a requires the co-expression of the NR2A subunit in transfected cells. Neuroscience 70:989–997. CrossRef Medline

Medzihradsky F, Ahmad K (1971) The uptake of pentazocine into brain. Life Sci I 10:711–720. Medline

Miller CL, Bickford PC, Luntz-Leybman V, Adler LE, Gerhardt GA, Freedman R (1992) Phencyclidine and auditory sensory gating in the hippocampus of the rat. Neuropharmacology 31:1041–1048. CrossRef Medline

Monnet FP, Debonnel G, Junien JL, De Montigny C (1990) *N*-methyl-D-aspartate-induced neuronal activation is selectively modulated by sigma receptors. Eur J Pharmacol 179:441–445. CrossRef Medline

Monnet FP, Debonnel G, Bergeron R, Gronier B, de Montigny C (1994) The effects of sigma ligands and of neuropeptide Y on *N*-methyl-D-aspartate-induced neuronal activation of CA3 dorsal hippocampus neurones are differentially affected by pertussin toxin. Br J Pharmacol 112:709–715. CrossRef Medline

Monnet FP, de Costa BR, Bowen WD (1996) Differentiation of sigma ligand-activated receptor subtypes that modulate NMDA-evoked [^{3}H]-noradrenaline release in rat hippocampal slices. Br J Pharmacol 119:65–72. CrossRef Medline

Morin-Surun MP, Collin T, Denavit-Saubié M, Baulieu EE, Monnet FP (1999) Intracellular sigma1 receptor modulates phospholipase C and protein kinase C activities in the brainstem. Proc Natl Acad Sci U S A 96:8196–8199. CrossRef Medline

Myers AM, Charifson PS, Owens CE, Kula NS, McPhail AT, Baldessarini RJ, Booth RG, Wyrick SD (1994) Conformational analysis, pharmacophore identification, and comparative molecular field analysis of ligands for the neuromodulatory sigma 3 receptor. J Med Chem 37:4109–4117. CrossRef Medline

Nebl T, Pestonjamasp KN, Leszyk JD, Crowley JL, Oh SW, Luna EJ (2002) Proteomic analysis of a detergent-resistant membrane skeleton from neutrophil plasma membranes. J Biol Chem 277:43399–43409. CrossRef Medline

Nguyen EC, McCracken KA, Liu Y, Pouw B, Matsumoto RR (2005) Involvement of sigma (sigma) receptors in the acute actions of methamphetamine: receptor binding and behavioral studies. Neuropharmacology 49:638–645. CrossRef Medline

Niethammer M, Kim E, Sheng M (1996) Interaction between the C terminus of NMDA receptor subunits and multiple members of the PSD-95 family of membrane-associated guanylate kinases. J Neurosci 16:2157–2163. Medline

Nishimura T, Ishima T, Iyo M, Hashimoto K (2008) Potentiation of nerve growth factor-induced neurite outgrowth by fluvoxamine: role of sigma-1 receptors, IP3 receptors and cellular signaling pathways. PLoS One 3:e2558. CrossRef Medline

Pláteník J, Balcar VJ, Yoneda Y, Mioduszewska B, Buchal R, Hynek R, Kilianek L, Kuramoto N, Wilczynski G, Ogita K, Nakamura Y, Kaczmarek L (2005) Apparent presence of Ser133-phosphorylated cyclic AMP response element binding protein (pCREB) in brain mitochondria is due to cross-reactivity of pCREB antibodies with pyruvate dehydrogenase. J Neurochem 95:1446–1460. CrossRef Medline

Quirion R, Bowen WD, Itzhak Y, Junien JL, Musacchio JM, Rothman RB, Su TP, Tam SW, Taylor DP (1992) A proposal for the classification of sigma binding sites. Trends Pharmacol Sci 13:85–86. CrossRef Medline

Salussolia CL, Prodromou ML, Borker P, Wollmuth LP (2011) Arrangement of subunits in functional NMDA receptors. J Neurosci 31:11295–11304. CrossRef Medline

Sans N, Petralia RS, Wang YX, Blahos J 2nd, Hell JW, Wenthold RJ (2000) A developmental change in NMDA receptor-associated proteins at hippocampal synapses. J Neurosci 20:1260–1271. Medline

Sanz-Clemente A, Nicoll RA, Roche KW (2013) Diversity in NMDA receptor composition: many regulators, many consequences. Neuroscientist 19:62–75. CrossRef Medline

Sato K, Saito Y, Kawashima S (1995) Identification and characterization of membrane-bound calpains in clathrin-coated vesicles from bovine brain. Eur J Biochem 230:25–31. CrossRef Medline

Schneider CA, Rasband WS, Eliceiri KW (2012) NIH Image to ImageJ: 25 years of image analysis. Nat Methods 9:671–675. CrossRef Medline

Standley S, Petralia RS, Gravell M, Hamilton R, Wang YX, Schubert M, Wenthold RJ (2012) Trafficking of the NMDAR2B receptor subunit distal cytoplasmic tail from endoplasmic reticulum to the synapse. PLoS One 7:e39585. CrossRef Medline

Steinfels GF, Alberici GP, Tam SW, Cook L (1988) Biochemical, behavioral, and electrophysiologic actions of the selective sigma receptor ligand (+)-pentazocine. Neuropsychopharmacology 1:321–327. Medline

Su TP, Hayashi T, Maurice T, Buch S, Ruoho AE (2010) The sigma-1 receptor chaperone as an inter-organelle signaling modulator. Trends Pharmacol Sci 31:557–566. CrossRef Medline

Suh YH, Terashima A, Petralia RS, Wenthold RJ, Isaac JT, Roche KW, Roche PA (2010) A neuronal role for SNAP-23 in postsynaptic glutamate receptor trafficking. Nat Neurosci 13:338–343. CrossRef Medline

Taha MS, Nouri K, Milroy LG, Moll JM, Herrmann C, Brunsveld L, Piekorz RP, Ahmadian MR (2014) Subcellular fractionation and localization studies reveal a direct interaction of the fragile X mental retardation protein (FMRP) with nucleolin. PLoS One 9:e91465. CrossRef Medline

Tchedre KT, Huang RQ, Dibas A, Krishnamoorthy RR, Dillon GH, Yorio T (2008) Sigma-1 receptor regulation of voltage-gated calcium channels involves a direct interaction. Invest Ophthalmol Vis Sci 49:4993–5002. CrossRef Medline

Villa A, Sharp AH, Racchetti G, Podini P, Bole DG, Dunn WA, Pozzan T, Snyder SH, Meldolesi J (1992) The endoplasmic reticulum of purkinje neuron body and dendrites: molecular identity and specializations for Ca2+ transport. Neuroscience 49:467–477. CrossRef Medline

Wanisch K, Wotjak CT (2008) Time course and efficiency of protein synthesis inhibition following intracerebral and systemic anisomycin treatment. Neurobiol Learn Mem 90:485–494. CrossRef Medline

Zambon AC, De Costa BR, Kanthasamy AG, Nguyen BQ, Matsumoto RR (1997) Subchronic administration of *N*-[2-(3,4-dichlorophenyl) ethyl]-*N*-methyl-2-(dimethylamino) ethylamine (BD1047) alters sigma 1 receptor binding. Eur J Pharmacol 324:39–47. CrossRef Medline

Zhang H, Cuevas J (2002) Sigma receptors inhibit high-voltage-activated calcium channels in rat sympathetic and parasympathetic neurons. J Neurophysiol 87:2867–2879. Medline

Zhang H, Cuevas J (2005) Sigma receptor activation blocks potassium channels and depresses neuroexcitability in rat intracardiac neurons. J Pharmacol Exp Ther 313:1387–1396. CrossRef Medline

Zhang H, Katnik C, Cuevas J (2009) Sigma receptor activation inhibits voltage-gated sodium channels in rat intracardiac ganglion neurons. Int J Physiol Pathophysiol Pharmacol 2:1–11. Medline

Zhang XJ, Liu LL, Jiang SX, Zhong YM, Yang XL (2011a) Activation of the sigma receptor 1 suppresses NMDA responses in rat retinal ganglion cells. Neuroscience 177:12–22. CrossRef Medline

Zhang XJ, Liu LL, Wu Y, Jiang SX, Zhong YM, Yang XL (2011b) sigma receptor 1 is preferentially involved in modulation of N-methyl-D-aspartate receptor-mediated light-evoked excitatory postsynaptic currents in rat retinal ganglion cells. Neurosignals 19:110–116. CrossRef Medline